Generalised drought index: A novel multi-scale daily approach for drought assessment

João António Martins Careto[1], Rita Margarida Cardoso[1], Ana Russo[1], Daniela Catarina André Lima[1], Pedro Miguel Matos Soares[1]

[1] Universidade de Lisboa,Faculdade de Ciências,Instituto Dom Luiz, 1749-016 Lisbon, Portugal.

Correspondence to: João Careto (jacareto@ciencias.ulisboa.pt)

Abstract. Drought is a complex climatic phenomenon characterised by water scarcity and is recognised as the most widespread and insidious natural hazard, posing significant challenges to ecosystems and human society. In this study, we propose a new daily based index for characterising droughts, which involves standardising precipitation and/or precipitation minus potential evapotranspiration data. The new index, the Generalised Drought Index (GDI), proposed here is computed for the entire period available from the Iberian Gridded Dataset (1971 to 2015). Comparative assessments are conducted against the daily Standardised Precipitation Index (SPI), the Standardised Precipitation Evapotranspiration Index (SPEI), and a simple Z-Score standardisation of climatic variables. Seven different accumulation periods are considered (7, 15, 30, 90, 180, 360, and 720-days) with three drought levels: moderate, severe, and extreme. The evaluation focuses mainly on the direct comparison amongst indices, in their ability to conform to the standard normal distribution, added value assessment using the Distribution Added Value (DAV) and a simple bias difference for drought characteristics. Results reveal that the GDI, together with the SPI and SPEI follow the standard normal distribution. In contrast, the Z-Score index depends on the original distribution of the data. The daily time step of all indices allows the characterisation of flash droughts, with the GDI demonstrating added value when compared to SPI and SPEI for the shorter and longer accumulations, with positive DAV up to 35%. Compared to the Z-Score, the GDI shows expected greater gains, particularly at lower accumulation periods, with DAV reaching 100 %. Furthermore, the spatial extent of drought for the 2004-2005 event is assessed. All three indices generally provide similar representations, except for the Z-Score, which exhibits limitations in capturing extreme drought events at lower accumulation periods. Overall, the findings suggest that the new index offers improved performance and adds value comparatively to similar indices with a daily time step.

1. Introduction

Drought is known to be one of the most impactful and costliest weather-related disasters, affecting the ecosystems, the economy, and sectors such as agriculture, health, and water management (Wilhite, 2000; Rhee et al., 2010; Vicente-Serrano et al., 2013; Wang et al., 2014; 2017; Lai et al., 2019). Amongst all natural disasters, droughts can spread further and have the most extend length (Jain et al., 2010), developing often in a slow manner, while at the same time, their effects can linger in the environment long after the end of the event (Vicente-Serrano et al., 2013; Hunt et al, 2014).

Over the years, numerous indices have been developed to assess drought conditions, particularly related to intensity and duration. One of the first proposed drought indices was the Palmer Drought Severity Index (PDSI, Palmer, 1965; Alley, 1984), which enables the measurement and evaluation of wet and dry conditions. The PDSI standardises the balance between monthly precipitation and atmospheric demand by incorporating potential evapotranspiration in its formulation. While this index was a landmark, it does have certain shortcomings. Its performance is enhanced only for the region where the index was initially defined with its outputs being heavily

influenced by the chosen calibration period. Therefore, PDSI revealed problems related to its spatial comparison and application. To address some of these issues, Wells et al. (2004) introduced the self-calibrated PDSI, which allows for spatial comparison and identifies extreme wet and dry events as rare occurrences. However, fixed timescales for computing the index remained a concern. Further developments were introduced during the following years to address these caveats. The Standardised Precipitation Index (SPI, McKee et al., 1993) is one of the indices developed which tackled the comparability and temporal scales issues (Guttman 1998; Hayes et al. 1999). SPI is a straightforward standardised index only requiring monthly precipitation, representing it as a standard deviation from its mean. SPI overcomes the limitations of the self-calibrated PDSI by enabling the computation of the index at various timescales. Nevertheless, SPI the sole use of precipitation could be a limiting factor depending on the climatic dominating conditions in certain regions. Moreover, with anthropogenic climate change, rising temperatures and the subsequent increases in evapotranspiration can also significantly increase the impact of drought events (Hu and Wilson, 2000; Vicente-Serrano et al., 2010). Therefore, including the influence of atmospheric evaporative demand in a drought index becomes imperative (Vicente-Serrano et al., 2010; Svoboda and Fuchs, 2016). To address this need, Vicente-Serrano et al. (2010) proposed the Standardised Precipitation Evapotranspiration Index (SPEI), which was further developed by Beguería et al. (2014). SPEI combines all the features and advantages of SPI together with the inclusion of atmospheric evaporative demand represented by the potential evapotranspiration. Both SPI and SPEI are indices that require data to be fitted to a theoretical Probability Density Distribution (PDF). In the literature, numerous PDFs have been considered. For SPI, distributions such as Pearson type III (Vicente-Serrano et al., 2006) or Gamma (Mkee et al., 1993; Edwards et al., 1997; Wang et al., 2022; Zhang et al., 2023) have been commonly employed. On the other hand, the 3-parameter log-logistic (Beguería et al., 2014; Wang et al., 2015; Ma et al., 2020) and the Generalised Extreme Value (Stagge et al., 2015; Wang et al., 2021; Zhang et al., 2023) distributions have been widely used for SPEI. However, the best distribution to fit the data is still not clear, as the same distribution may perform differently for distinct regions (Stagge et al., 2015; Monish and Rehana, 2020; Zhang and Li, 2020). For instance, for a global dataset, Stagge et al. (2015) concluded that the Gamma (Weibull) for long (short) accumulations was the best distribution for SPI, while the Generalised Extreme value was the best distribution to fit SPEI. On the other hand, Zhang and Li. (2020), concluded that the Log-Logistic distribution could be used as an alternative when analysing SPI for a large river basin in China. At the same time, the Log-logistic distribution which is known to be resilient to the presence of outliers (Ahmad et al., 1988) and more appropriate for the Iberian Peninsula (Vicente-Serrano et al., 2010; Beguería et al., 2014), was deemed the best function for fitting the data for SPEI. Usually, the SPI and SPEI indices only rely on a single probability density distribution, even for large regions. To overcome this issue, there are methods to estimate the underlying distribution and associated parameters, which could, however, become computationally infeasible for large datasets (Guttman, 1999). At the same time, the method considered to estimate the parameters of a single distribution could also be computationally demanding.

Simpler drought indices which do not require fitting to a distribution also exist. One is the Z-Score which is computed for precipitation or with the difference between precipitation and evapotranspiration by subtracting the long-term mean and dividing the result by the long-term standard deviation (Umran Komuscu, 1999; Patel et al.,

2007; Akhtari et al., 2009; Jain et al., 2015). Slightly different formulations for this index also exist such as those used by Zhang et al. (2022a) and (2022b), or the China Z-Index (Wu et al., 2001) and is also considered in the standardised Reconnaissance Drought Index (Tsakiris and Vangelis, 2004). The advantage of the Z-Score index lies in its simple calculation being considered an alternative to indices which require fitting data to a distribution such as the SPI or SPEI, being capable of accommodating missing values. Similarly, the Z-Score also represents a standardised departure from the mean. However, the Z-Score may not effectively represent the shorter timescales since precipitation data is skewed (Edwards, 1997). Additionally, the index's performance may vary in regions with diverse precipitation or potential evapotranspiration patterns, where data does not assume a normal distribution. This can affect the accuracy and reliability of the index.

Although droughts are, in general, known to be a slowly evolving phenomenon (Wilhite and Glantz, 1985; Mishra and Singh, 2010), recently the concept of flash drought has emerged (Wang et al., 2021;2022; Zhang et al., 2022a; Christian et al., 2023). These types of extreme events are characterised by a sudden onset, fast aggravation, and end (Christian et al., 2023). Depending on the type of climate, these short-duration events may threaten the water supply and cause significant reductions in crop yield at critical stages of plant development (Meyer et al., 1993; Dai, 2011; Vicente-Serrano et al., 2013; Hunt et al., 2014). due to their sub-monthly timescale nature flash droughts can only be identified with daily drought indices. Therefore, the widespread of observational-based daily gridded datasets such as the National Gridded Dataset for the Iberia Peninsula (IB01; Herrera et al., 2019), Climate Prediction Center (CPC, Xie et al., 2007; Chen et al., 2008), the E-OBS (Cornes et al., 2018), the European Meteorological Observations (EMO-5, Thiemig et al., 2022), station based datasets such as the European Climate Assessment & Dataset (ECA&D, Klein-Tank et al., 2002), reanalysis data such as ERA5 (Hersbach et al., 2020; 2023), the JRA-55 (Kobayashi et al., 2015), the Merra-2 (Gelaro et al., 2017), or regional climate models initiatives such as the World Climate Research Program Coordinated Regional Climate Downscaling Experiment (CORDEX, Giorgi et al., 2009; 2021, Gutowski et al., 2016), assisted in the development of new drought indices with a daily time step (Wang et al., 2015; 2021; 2022; Jia et al., 2018; Li et al., 2020; Ma et al., 2020; Onuşluel Gül et al., 2021; Zhang et al., 2022a; 2022b; Zhang et al., 2023). At the same time, most of these indices are still fitted to a probability distribution and/or are not standardised. Wang et al. (2015) used a daily version of SPEI to understand if there has been any improvement in drought conditions. The authors report that the daily SPEI can provide a more comprehensive understanding of drought dynamics at a finer temporal scale. Li et al. (2020) proposed the Standardised Antecedent Precipitation Evapotranspiration Index. The index is first compared against the monthly PDSI, SPEI and soil moisture, revealing a similar performance against SPEI at the monthly scale while outperforming at the weekly scale. Ma et al. (2020) computed a daily SPEI index and compared it with the traditional monthly version. The authors reported that the daily index can capture more detailed drought events than the monthly counterpart. Wan et al. (2023) also considered a daily SPEI index to determine the trend of drought severity and duration over 40 years (1979-2018) for China. The authors also concluded that the potential evapotranspiration was the dominant climatic factor influencing drought for most of the region. Zhang et al. (2022a) proposed the Daily Evapotranspiration Deficit Index and compared the results against the Meteorological Drought Composite Index and SPEI for four drought events in China. The proposed index was able to capture

better the start and end of the events, as well as the peak intensity. Still, indices such as the SPI or the SPEI computed at the daily scale also prove to be demanding. The parameter estimation and the subsequent fitting to a theoretical distribution may be computationally expensive and result in a poor fit. At sub-monthly aggregation scales, the presence of outliers could hinder the parameter estimation and fit andgenerate values that might fall outside the range of the chosen distribution. Furthermore, periods with no precipitation may also pose difficulties in computing the SPI index (Beguería et al., 2014). Table 1 displays a summary of all indices presented here.

Nevertheless, daily indices are still at an early stages in comparison with the diverse monthly drought indices available. Motivated by the shortcomings illustrated before, in the present study, we propose a new daily drought index, the Generalised Drought Index (GDI). The GDI is an index identical to SPI or SPEI in the sense of standardising data to follow the standard normal distribution, allowing the evaluation of both short and long-time-scale droughts with a daily time step. Furthermore, GDI allows for a generalised fitting distribution which is empirically based, and thus the index accepts alternative variables for drought assessment and not only precipitation. For instance, actual evapotranspiration could be considered as an alternative to the usual precipitation minus potential evapotranspiration (P-PET). Moreover, the new index may be perceived as an alternative for removing skewness and kurtosis from climate data. Here, the GDI index is computed for the Iberian Peninsula region using the IB01 dataset, covering 1971-2015. Our study contributes to the ongoing efforts to develop more effective drought monitoring tools and provides a valuable instrument for decision-makers and stakeholders to better manage the impacts of flash-droughts and longer droughts, consistently and solidly. Our proposed index can be easily implemented in regions with limited climatic variables and can help improve the accuracy and reliability of drought assessment, requiring solely long-time series. The introduction of GDI can also be regarded as an important step in the evaluation of climate simulations. This is particularly relevant for high-resolution models such as those from the EURO-CORDEX (Jacob et al., 2014; 2020; Gutowski et al., 2016) or from the CORDEX flagship FPS-Convection simulations (Coppola et al., 2020; Ban et al., 2021; Pichelli et al., 2021), which aim to capture extreme weather events more accurately than their coarser counterparts. With the use of daily datasets and a daily drought index, researchers can more accurately assess a model's ability in capturing the fast-evolving conditions, characteristic from flash-droughts. Therefore, the GDI allows for a better understanding of drought dynamics, facilitating the evaluation of not only long-term drought events but also short-term variability. Furthermore, with GDI index one can more easily perform studies of co-occurrence with other types of extremes such as heatwaves or fire ignitions (Zscheischler et al., 2020; Shan et al., 2024), all on the same scale.

The following section introduces the IB01, as well as the methodology for computing the GDI, the SPI and SPEI, and finally the simple Z-Score standardisation. Afterwards, the results are presented in section 3, followed by a Discussion and Conclusions in section 4.

Table1. Examples of drought indices.

Index	Reference	Aggregation			Variable			Method		
------	------	Monthly	Weekly	Daily	PR	PR-PET	AET	Fit to Dist.	Empirical Fit	Equation
PDSI	Palmer, (1965)	X				X				X
sc-PDSI	Wells et al. (2004)	X				X				X
SPI	Mckee et al. (1993) Zhang et al. (2023)	X		X	X			X		
SPEI	Vicente-Serrano et al. (2010) Ma et al. (2020) Zhang et al. (2022a)	X	X	X		X		X		
Z-Score	Komusou, (1999)	X	X	X		X				X
RDI	Tsakiris and Vangelis, (2004)	X				X				X
SAPEI	Li et al. (2020)	X	X			X		X		
DEDI	Zhang et al. (2022a)			X		X		X		
GDI	------	X	X	X	X	X	X			X

2. Data and Methods

2.1. Study Area

The Iberian Peninsula exhibits a diverse and complex climate influenced by its geographical position, surrounded by the Atlantic Ocean to the north and west and the Mediterranean Sea to the south and east. In the northern

regions of the Iberian Peninsula, such as Galicia and northern Portugal, a maritime climate prevails, characterised by mild winters and cool summers. The Atlantic Ocean influence brings relatively high precipitation throughout the year (Rios-Entenza et al., 2014). Towards the south, the climate shifts to a more Mediterranean type, with hot and dry summers. Winters remain mild and relatively wet compared to the summer months. The Mediterranean climate is associated with distinct wet and dry seasons, with most rainfall occurring during the winter (Peel et al., 2007). Droughts are a recurring and significant challenge for the Iberian Peninsula. The region has a long history of drought events, with a clear drying trend throughout the 20th century, mainly due to increased temperature (Fonseca et al., 2016; Páscoa et al., 2021). Climate change projections suggest that the frequency and intensity of droughts may amplify in the future (Sanchez et al., 2011; Seguí et al., 2016; Moemken et al., 2022; Soares et al., 2023a). Rising temperatures and changing precipitation patterns may exacerbate water scarcity and put additional stress on the region's ecosystems. (Soares et al., 2017; Cardoso et al., 2019; Carvalho et al., 2021; Soares and Lima 2022).

2.2. IB01 Observational Dataset

The IB01 Observational dataset (Herrera et al., 2019) is a high-quality dataset that offers daily values for precipitation, as well as minimum and maximum temperatures, with a spatial resolution of 0.1^{o}. This dataset was constructed using an extensive network of quality-controlled observational weather stations (a maximum of 3486 for precipitation and 275 for temperatures) across the Iberian Peninsula from 1971 to 2015. Herrera et al. (2019) reported that not only IB01 effectively captures the spatial patterns of the mean and extreme precipitation and temperatures. but also exhibits a more realistic precipitation pattern than E-OBS (Cornes et al., 2018), and comparable performance to E-OBS for temperatures.

The IB01 dataset has been employed in numerous studies to characterise the present climate and was used as a benchmark for evaluating the ability of a set of EURO-CORDEX (Giorgi et al., 2009; Jacob et al., 2014; 2020; Gutowski et al., 2016) simulations to reproduce the present climate over Iberia (Herrera et al. 2020; Páscoa et al., 2021; Careto et al., 2022a; 2022b; Lima et al., 2023a; 2023b; Soares et al., 2023b). Herrera et al. (2020) evaluated the performance of the EURO-CORDEX over the Iberian Peninsula and characterised the observational uncertainty with the use of the IB01, E-OBS-v19e, and MESAN-0.11^{o} datasets. Páscoa et al. (2021) employed this dataset to assess the recent trends in drought events across Iberia. Careto et al. (2022a) and (2022b) evaluated the added value of using high-resolution simulations from EURO-CORDEX in characterizing means and extremes of precipitation and temperature over the Iberian Peninsula. More recently, Lima et al. (2023a) considered the IB01 dataset as the reference to evaluate the accuracy of a set of historical EURO-CORDEX simulations in representing the main properties of the observed climate within mainland Portugal. Based on this evaluation, a weighted multi-variable multi-model ensemble of EURO-CORDEX simulations was built and used to characterise both the mean climate, extremes, and indices (Lima et al. 2023a and 2023b), as well as water scarcity conditions over Portugal (Soares and Lima, 2022) throughout the 21st century. Based on the same weighting methodology, Soares et al. (2023b) projected the future of drought events across the Iberian Peninsula. Finally, IB01 was used to critically assess the CMIP quality to project the recent past climate of Iberia (Soares et al, 2023a).

2.3. Potential Evapotranspiration

Potential Evapotranspiration (PET) represents the maximum atmospheric water demand and is a requirement for the computation of several drought indices (Vicente-Serrano et al., 2010; Li et al., 2020; Zhang et al., 2022a; 2022b). The FAO-56 Penman-Monteith formula (Allen et al., 1998) is one of the most widely used approaches to calculate PET. Although it was specifically designed for non-stressed grass cover, is considered the most accurate estimate. However, it requires multiple variables, some of which may not be readily available, posing a drawback to its practical implementation. An alternative approach, known for its simplicity, is the Thornthwaite formulation (Thornthwaite, 1948), which only requires latitude and temperature as inputs. However, studies have shown that the Thornthwaite formulation underestimates PET in arid and semiarid regions while overestimating it in humid tropical or equatorial regions (van der Schrier et al., 2011). Therefore, in the context of climate change and the Iberian Peninsula, with arid and semiarid regions, this equation is not the best option for computing PET (Beguería et al., 2014)

As a compromise between formulation complexity and data availability, a modified version of the Hargreaves formulation is thus considered in this study (Droogers and Allen, 2002). The Modified Hargreaves is identical to the original Hargreaves method, in which beyond the incorporation of maximum and minimum temperature, the precipitation is also integrated. Precipitation data is commonly accessible in most modelling and observational datasets and can serve as a proxy for cloud cover and humidity. In this study, a daily version of the Modified Hargreaves formula is implemented (Farmer et al., 2011):

$$PET = 0.0019 * 0.408 * RA * (Tavg + 21.0584)(TD - 0.0874 * P)^{0.6278} \quad (1)$$

More details on the calculation of the PET with the modified Hargreaves version can be found in Soares et al. (2023).

2.4. Drought Indices

2.4.1. Standardised Precipitation and Standardised Precipitation Evapotranspiration Indices

In this section, the Standardised Precipitation Index (SPI, McKee et al. 1993) and the Standardised Precipitation Evapotranspiration Index (SPEI, Vicente-Serrano et al. 2010) are presented. Both SPI and SPEI are commonly used (Edwards, 1997; Vicente-Serrano et al. 2006; 2010; Beguería et al. 2014; Wang et al. 2022; Zhang et al. 2022a; 2022b) with the former being calculated based solely on precipitation (hereafter PR) and the latter on a simplified water balance (Precipitation minus Potential Evapotranspiration, hereafter PR-PET). Probabilistic indices such as these allow for a Standardised juxtaposition and comparison across different spatial areas or between climate zones (Vicente-Serrano et al., 2010; Pohl et al., 2023)

To compute either the SPI or the SPEI, first, the PR and PR-PET data must be aggregated into the desired timescale through a moving window with a length equal to the timescale, i.e., a daily value is computed as the sum of the day under analysis (d) and the previous $s - 1$ days where s is the timescale (in days):

$$X_d = \sum_{d-(s-1)}^{d} data \quad (2)$$

Subsequently, a daily yearly mean is obtained from a moving window of 31 days centred on each day d:

$$Se = \frac{1}{31Y}\sum_{i=1}^{Y}\sum_{j=D-15}^{D+15} X_{d_{i,j}} \quad (3)$$

Where Y is the total number of years and D is the day of the year. For instance, 1st January corresponds to day 1 and 31st December to day 366. To ease all computations, all years are considered to have 366 days in order to include the 29th of February from leap years. Consequently, the value for 29th February from non-leap years is considered a missing value. Thus, Se is an annual mean cycle. Thirdly, this annual cycle is removed from the X_d series:

$$X_a = \sum_{i=1}^{Y}\sum_{j=1}^{366} X_{d_{i,j}} - Se_j \quad (4)$$

Traditionally, the removal of the seasonal cycle is not performed for the SPI and SPEI. However, it can be regarded as a step to remove days without precipitation, which is relevant in the case of the SPI index. Usually in those situations, a factor is considered for precipitation data (Stagge et al., 2015; Wang et al., 2022; Zhang et al., 2023).

Afterwards, the X_a series are adjusted to a theoretical distribution. The log-logistic distribution (Eq- 5) was chosen to fit X_a for both SPI (Zhang and Li, 2020) and SPEI (Vicente-Serrano et al., 2010; Beguería et al., 2014). Therefore, the difference between the two indices lies solely in the inclusion of PET for SPEI. To avoid issues when fitting the data to the distribution, first the values of the X_a series are shifted to positive values above 0. This change does not affect the distribution or the final value. $f(x) = \frac{\beta}{\alpha}\left(\frac{x-\gamma}{\alpha}\right)^{\beta-1}\left[1+\left(\frac{x-\gamma}{\alpha}\right)^{\beta}\right]^{-2}$ (5)

The three parameters β (shape), α (scale) and γ (location) can be estimated via the maximum likelihood or with Probability Weighted Moments (PWM, Hosking, 1986; 1990). Following Beguería et al. (2014), the unbiased estimator for PWM (Hosking, 1986) was considered:

$$W_s = \frac{1}{N}\sum_{i=1}^{N}\frac{\binom{N-i}{s}}{\binom{N-1}{s}}X_{d_i} = \frac{1}{N}\sum_{i=1}^{N}\frac{\Gamma(\mathrm{N}-\mathrm{i}+1)/(\Gamma(\mathrm{s}+1)\Gamma(\mathrm{N}-\mathrm{i}-\mathrm{s}+1)}{\Gamma(\mathrm{N})/(\Gamma(\mathrm{s}+1)\Gamma(\mathrm{N}-\mathrm{s}))}X_{a_i} \quad (6)$$

Moments W_s of different orders s can be computed easily via software programming tools. Γ denotes the gamma function for Natural numbers including 0. From the first three moments (W_0, W_1 and W_2) it is possible to obtain the three parameters for the Log-Logistic (Singh et al., 1993):

$$\beta = \frac{2W_1 - W_0}{6W_1 - W_0 - 6W_2} \quad (7)$$

$$\alpha = \frac{(W_0 - 2W_1)\beta}{\Gamma\left(1+\frac{1}{\beta}\right)\Gamma\left(1-\frac{1}{\beta}\right)} \quad (8)$$

$$\gamma = W_0 - \alpha\Gamma\left(1+\frac{1}{\beta}\right)\Gamma\left(1-\frac{1}{\beta}\right) \quad (9)$$

To convert the X_a series into SPI or SPEI, the Cumulative Distribution Function (CDF) of the Log-Logistic is required to obtain the accumulated probability:

$$F(x) = \left[1+\left(\frac{\alpha}{X_a-\gamma}\right)^{\beta}\right]^{-1} \quad (10)$$

Having the accumulated probabilities, the indices can be easily obtained following the classical approximation of Abramowitz and Stegun. (1965):

$$P = 1 - F(x) \quad (11)$$

$$P = 1 - P, if\ P > 0.5 \quad (12)$$

If P is above 0.5, then the signal of the final index is also reversed.

$$W = \sqrt{-2\ln(P)} \quad (13)$$

$$SPEI = W - \frac{C_0 + C_1 W + C_2 W^2}{1 + D_1 W + D_2 W^2 + D_3 W^3} \quad (14)$$

With $C_0 = 2.515517, C_1 = 0.802853, C_2 = 0.010328, D_1 = 1.432788, D_2 = 0.189269\ and\ D_3 = 0.001308$.

2.4.2. Z-Score Index

Z-Score method is a straightforward approach used to standardise a dataset based on its mean and standard deviation (Umran Komuscu, 1999; Patel et al., 2007; Akhtari et al., 2009; Jain et al., 2015). It follows a simple rationale: 1) obtain the accumulated series and remove its seasonal cycle, as described in section 2.4.1; 2) remove the mean and divide the result by the standard deviation to get the X_a anomalies. This ensures that all data points have the same statistics for mean and standard deviation. However, it is important to note that while the mean and standard deviation will be consistent across all points, the underlying distribution and its parameters describing the data at each location may vary. Still, for long accumulations and as a consequence of the central limit theorem, the Z-Score and the standardised indices approach each other. The Z-Score can be computed by:

$$Z - Score = \frac{X_a - \overline{X_a}}{\sigma(X_a)} \quad (15)$$

2.4.3. Generalised Drought Index

A new index, the Generalised Drought Index (GDI) is proposed here as an alternative to the commonly used Standardised drought indices, such as the SPI or the SPEI, both described in section 2.3.1. The GDI is also a standardised index but introduces three upgrades which are particularly interesting when addressing drought impacts that often occur at sub-monthly scales:

- It can be calculated using any daily aggregation. For instance, the 7-, 15-, 30-, 90-, 180-, 360-, and 720-days were chosen, ranging from weekly to biannual aggregations. Regardless of the timescale chosen, a daily index is obtained, allowing an assessment of flash droughts, which were not possible with monthly indices.

- Since fitting to a distribution is not required, any variable relevant to drought characterisation can be considered as input, such as PR or PR-PET, actual evapotranspiration or PR divided by PET.
- Relies on a unique spline adjustment technique to smooth the cumulative histogram. The main advantage is the automatic fit of the empirical distribution to the data for different sites, resulting in an enhanced index.

Figure S2 (in the supplemental material) shows the two sample Cramér-von Mises statistics from all land points and for each accumulation period, comparing the GDI, SPI and SPEI cumulative distribution against the empirical cumulative distribution. This figure reveals that the spline adjustment outperforms the theoretical log-logistic fit used by both SPI and SPEI, as given by the lower values of the Cramér-von-Mises statistics across all time scales. Moreover, the p-value over the assumption that the H_0 hypothesis, where both samples came from the same distribution, cannot be rejected for the spline adjustment at the 5% significance level. This result is expected since the spline is empirically driven. However, in the case of SPI and SPEI the hypothesis H_0 is rejected for most accumulations where both samples came from different distributions. Again, this result is expected since the log-logistic distribution was assumed and used to fit the data, which for most cases does not correspond to the underlying distribution of the data.

To compute the GDI, the X_a series anomalies obtained in subsection 2.3.1 are considered. The following step is to compute a histogram of the data. The Freedman-Diaconis rule is used, which gives an optimised estimate for the bin width based on the data variability and length:

$$inc = 2 * \frac{IQR}{\sqrt[3]{N}} \tag{16}$$

Where IQR is the interquartile range and N is the length of the X_a series. The histogram is defined between the minimum and maximum values and is tailored specifically for each time series. Following Soares and Cardoso, (2018) the histogram series are normalised by the sum of all bins:

$$X_d = \frac{hist(X_d)}{\mathrm{sum}\big(hist(X_d)\big)} \tag{17}$$

$$X_d = S_N = \sum_{i=1}^{N} X_{d,i} * (1 - N^{-1}) \tag{18}$$

Subsequently, a cumulative sum of each bin is considered (Eq. 18). At this stage, the bins of the cumulative histogram were treated as data (x, y) points, where x represents the endpoint between the bin edges and y represents the corresponding probability. It is important to avoid 0s and 1s, since the cumulative distribution of the normal distribution tends to infinity for a probability of 0 and 1. Therefore the factor $(1 - N^{-1})$ was considered, slightly scaling down the value for all bins. A value proportional to the length of data $(1/N)$ was also appended at the minimum edge of the first bin, corresponding to the minimum value of the x_d series. Afterwards, a cubic spline technique (Fritsch and Butland, 1984) is used to smooth the cumulative histogram. With this approach the probability of any value can occur, without the need of a theoretical distribution fit.

This method allows the estimation of intermediate probabilities between the cumulative histogram points, resulting in a continuous and smooth representation of the underlying distribution, bounded by the probability of the minimum value $(1/N)$ and the last bin, allowing the preservation of the daily time step for the final index.

Afterwards, the original X_a series are converted into accumulated probabilities using the interpolated accumulated histogram. By using the inverse of the normal distribution, one can transform these probability values into a standardised series following the standard normal distribution with a mean of 0 and a standard deviation of 1. It is important to note that the feasibility of this approach depends on the length of the original time series, as the statistics from longer time series will tend to align more closely with the parameters of the normal distribution. This is identical to what occurs for both SPI and SPEI (McKee et al., 1993; Pohl et al., 2023). Figure 1 introduces a flowchart to guide the users on the steps needed to obtain the GDI.

2.5. GDI Evaluation

The performance of GDI, SPI, SPEI, and Z-Score is assessed using the IB01 dataset for each single location to generate quantile-quantile plots, which allows us to determine the underlying distribution of all-time series relative to the standard normal distribution. The percentiles considered for evaluation are constituted by a sequence from the 10^{th} to the 90^{th} percentile, with increments of 10. With this inter-comparative analysis, one can inspect the underlying distribution of the data and how close it is to the theoretical standard normal distribution. A wider vertical spread represents deviations of the time series from normality (linear line). Conforming results to the standard normal distribution is paramount in various statistical analyses, as it facilitates meaningful comparisons and allows for the application of well-established statistical techniques. When data closely follows the standard normal distribution, it exhibits known statistical properties, simplifying the interpretation of the results (e.g., equal mean and median, 68% of the data falls within one standard deviation of the mean, 95% of the data falls within two standard deviations of the mean). In the context of drought indices, compliance with normality assumptions is crucial for accurately characterising drought severity and frequency. Moreover, the standard normal distribution allows for direct comparison across different spatial areas and periods, which is particularly relevant for assessing drought severity and patterns on both regional and global scales (Guttman 1998; Hayes et al., 1999; Vicente-Serrano et al., 2006; 201; Beguería et al., 2014). As a complement, statistics including the mean, median, standard deviation, interquartile range, skewness, Yule-Kendall skewness, and kurtosis were computed for all indices, from all land points of observations.

A Distribution Added Value (DAV, Soares and Cardoso, 2018) assessment is also performed. In this version, the DAV allows a comparison and quantification of the similarity between distributions of the different indices to the standard normal distribution. This assessment is performed for the GDI against the SPI or SPEI and against the GDI against the Z-Score for each land grid point. To compute the DAV, a histogram is first constructed.

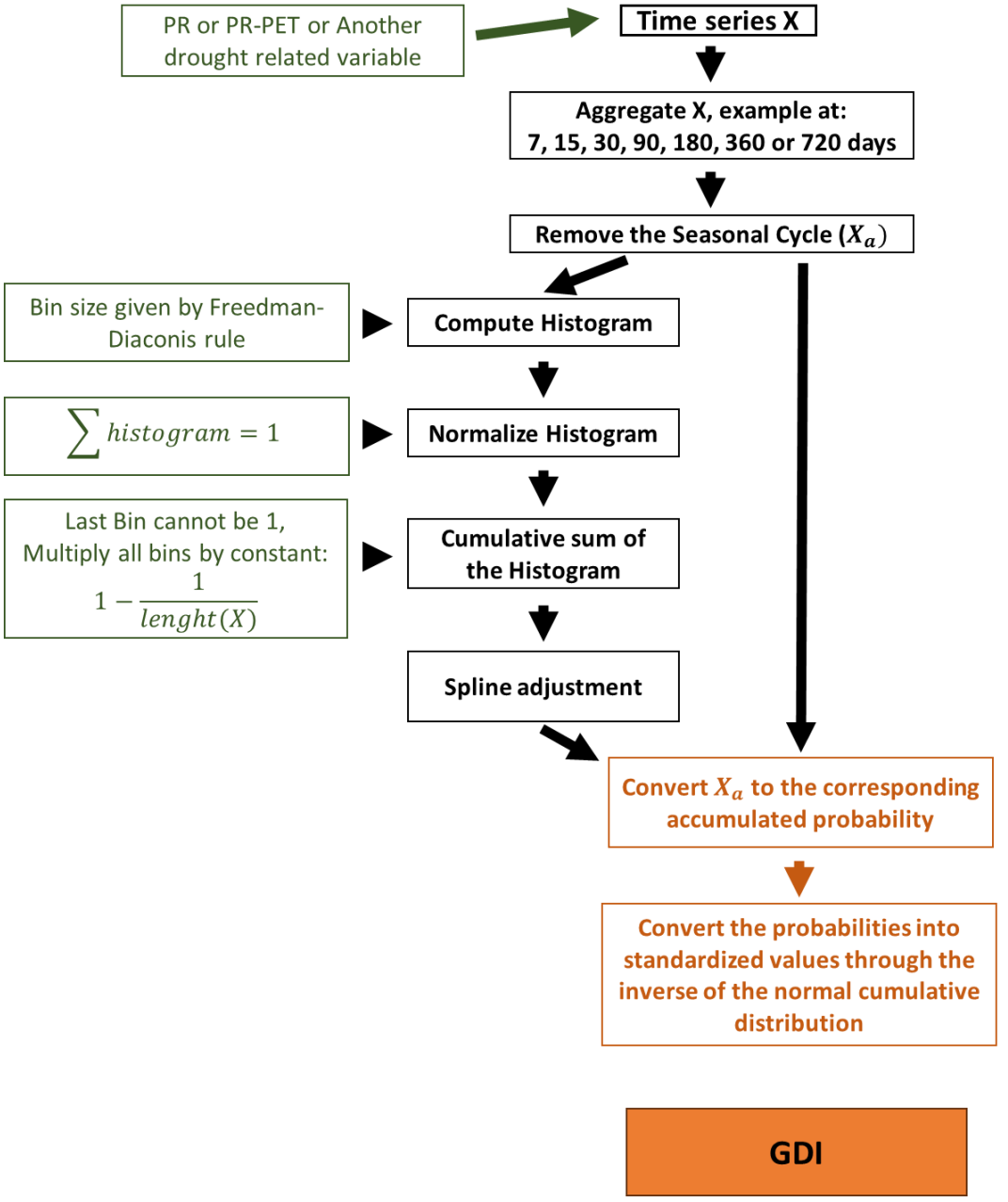

Figure 1. Flowchart for the construction of the Generalised Drought Index.

For GDI, SPI and SPEI the limits considered are -5 to 5, while for the Z-Score the limits are wider, ranging from -15 to 15. The bin width was set to be constant for all datasets and is determined by the Freedman-Diaconis rule described earlier. In this context, the 75th and 25th percentiles are taken from the theoretical standard normal distribution. To build the histogram of the normal distribution, the normalised rank of each time series is first considered (this is equivalent to the empirical CDF probabilities). The probabilities range from 0 to 1, where the first value is close to $1/N$ and the last value is $1 - 1/N$, where N corresponds to the data length at each location.

The factor used in eq. 17 is also contemplated here. These probabilities are then converted into values by considering the inverse of the standard normal distribution. Afterwards, each histogram is normalised by dividing each bin by the sum of all bins. From the histograms, a Perkins Skill Score (S_{index}; Perkins et al., 2007) is thus computed, which represents the sum of the lowest value of the two normalised histograms:

$$S_{index} = \sum^{\square}_{\square} min\left(normhist_{normal}, normhist_{index}\right) \quad (19)$$

where $normhist_{normal}$ is the normalised histogram for the normal distribution, the $normhist_{index}$ is the normalised histogram for a specific index. A score is computed for each individual index and represents the degree of similarity between the index histogram to the standard normal distribution histogram. The Perkins Skill Score of each index is then used to compute the DAV:

$$DAV = 100 * \frac{S_{GDI} - S_{index}}{S_{index}} \quad (20)$$

Where S_{index} is the score obtained for the SPI, SPEI or Z-Score. A positive percentage denotes an added value from the proposed GDI index. Finally, the Pearson correlation and Root-Mean-Squared-Error (RMSE) are also computed to further investigate the differences between the GDI and the other indices. All the metrics mentioned to this aimed to assess the overall performance for daily time series.

Regarding the drought characteristics, several aspects are examined such as the mean event severity, decadal frequency, mean event duration and daily spatial drought extent. The drought levels considered are as follows: moderate drought with an index below -0.5, severe drought with an index below -1 and extreme drought with an index below -1.5 (McKee et al., 1993; Soares et al., 2023b). The drought frequency can be defined as the average number of times any index falls below the specified threshold per decade. Mean event severity is computed by dividing the sum of all days with the index below the defined thresholds, against the total number of events. The mean event duration is computed similarly and is defined as the ratio between the total number of days by the total number of drought events. These drought characteristics are computed following Spinoni et al. (2018) and Soares et al. (2023). All the statistics were computed for all indices and for the 7-, 15-, 30-, 90-, 180-, 360- and 720 timescales considering each land grid point. A comparison is then performed by studying the spatial correlation and root mean squared error between the GDI and other indices, for moderate drought only. An assessment of the differences between the GDI against the SPI or SPEI and Z-Score is also performed, considering the drought characteristics. Additionally, the supplementary material includes comparisons of the GDI index against the monthly SPI and SPEI version computed with the default definitions provided by the 'SPEI' package for the R programming language (Beguería et al., 2014) as a complement. Whenever it is applied, the monthly GDI is also computed by aggregating the daily index at monthly time steps, by simply averaging the daily index. An analysis of the spatial extent of drought classes (moderate, severe, and extreme) is performed for the IB01 dataset for a case study. The spatial extent is computed for each day and is defined as a percentage of land points with any index below the given thresholds. This analysis is performed for the extreme drought that affected the Iberia Peninsula in 2004 and 2005, where the evaluation period corresponds to two hydrological years, starting in

October 2004 and ending in September 2006. Moreover, the spatial average time series of all drought indices for all time aggregations were also analysed.

3. Results

3.1. GDI General Performance

GDI, SPI and SPEI indices (Figs. 2a to 2d) reveal percentiles close to those obtained by a normal distribution. Figure 2a displays the results for the GDI computed solely from precipitation. For the timescales below 90 days, the distributions deviate slightly from the normal, particularly near the median. While, for the longer aggregation scales, the time series deviates more from the normal distribution towards the tails. Figure 2b, for the GDI computed with PR-PET, reveals a similar pattern. Yet, with the inclusion of PET, the deviations from the normal distribution are reduced. For SPI (Fig. 2c), the time series still follows the central line, although with a notorious dispersion. The pattern of the spread from all distributions remains similar for all accumulation scales, with higher deviations towards the tails of the distribution. For SPEI (Fig. 2d), the inclusion of PET relative to the SPI (Fig. 2c) did improve the results as in Fig. 2b for the GDI, but the pattern of spread remains rather large. Both SPI and SPEI present a larger spread in comparison to GDI. In the Z-Score index with PR (Fig. 2e) and PR-PET (Fig. 2d), the underlying distribution does not necessarily have to align with the normal standard distribution. Yet, due to the central limit theorem, for longer accumulations the time series tend towards normality, as evidenced by the alignment with the central line, despite the expected and large spread amongst all-time series. Figure S3 in the supplementary material shows the same but for the monthly versions of the GDI, SPI and SPEI indices. Although the spread is larger for the monthly GDI in comparison to the daily version, it is still lower than the SPI and SPEI indices.

As a complement, Fig. S4, in supplementary material, displays the statistics for all accumulation timescales and indices. The proximity of the values to zero indicates their similarity to the reference standard normal distribution. For the GDI indices, the mean and the median exhibit closer values, albeit with a slight deviation above 0. Nevertheless, those results together with the low skewness and kurtosis are good indicators of normality. For the SPI and SPEI indices, all metrics are near 0, although there is a more noticeable deviation among the time series in comparison with the results obtained for the GDI. Conversely, by definition, the Z-Score displays a mean of 0 and a standard deviation of 1. Still as expected from the statistics and the quantile-quantile plot from Fig. 2, the underlying distribution clearly deviates from normality.

To assess the performance of the new index, the DAV metric (Eq. 20) is applied (Table 2). In this configuration, the DAV metric allows a quantification of a higher or lower degree of conformity to the standard normal distribution, relative to the other indices. The Perkins Skill Scores are determined for GDI, SPI, SPEI and Z-score for each location individually and chosen time scales. Table 2a shows the DAV for GDI with PR against SPI, and GDI with PR-PET against SPEI. For each accumulation period, a histogram represents the percentage of land points within each DAV category. All locations for all accumulations clearly display positive added value. For most of the accumulation periods, more than 50 % of land points reveal gains between a DAV of 5 to 10 %.

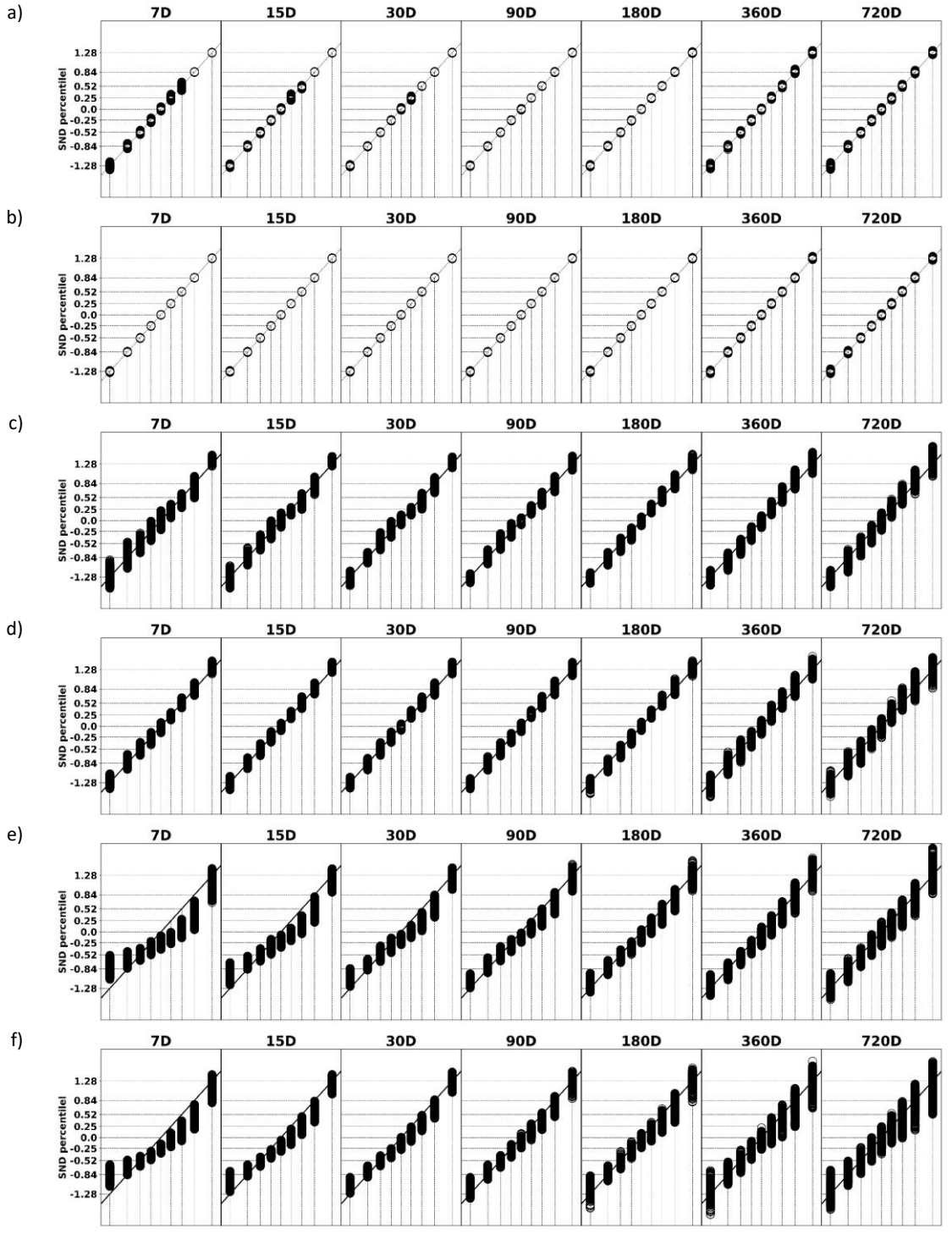

Figure 2. Quantile-Quantile plot against the 10th, 20th, 30th, 40th, 50th, 60th, 70th, 80th and 90th percentile from the standard normal distribution for all grid points of IB01 dataset for (a) GDI (PR), (b) GDI (PR-PET), (c) SPI, (d) SPEI, (e) Z-Score index (PR) and (f) Z-Score index (PR-PET). All indices were computed at the daily time step. A smaller vertical spread indicates a better agreement with the standard normal distribution from all locations. The numbers of the y-axis, the horizontal and vertical lines correspond to the percentiles of the standard normal distribution (SND percentile).

The exceptions are for 7 days accumulation for the PR indices and 720 days for the PR-PET, where most locations exhibit higher gains. However, the intermediate aggregation time scales (30D, 90D and 180D) still reveal more than 20 % of locations falling within the neutral DAV range (-5 to 5 %) for the PR indices. A similar trend occurs for the PR-PET indices, albeit with a more prominent result, with approximately 64 %, 48.5 % and 16.4 % of locations for the aggregations of 30-, 90-, and 180-days, respectively, having DAV values up to 5 %. Following Fig. 2, this behaviour is likely attributed to the PR-PET indices offering a better representation of the normal distribution. In general, GDI can add value, due to its improved representation of the shape of the cumulative distribution and consequently normality, as indicated in Fig. 2 and S4. Table 2b displays the DAV metric between the GDI and the Z-Score, showing that the GDI index reveals again a positive added value. In this case, since the underlying distribution for the original time series does not necessarily have to follow the normal distribution, large DAV values are expected. The gains are relevant, namely for the shorter accumulations. Towards the longer accumulations, the time series for the Z-Score better aligns with the normal distribution as hinted by Fig. 2e and 2f, returning lower DAV values. These findings are relevant and could indicate that the fit of the data to a chosen theoretical distribution could introduce some uncertainty into the final index, while a fit to an empirical distribution can return more precise results. Table S1 displays the DAV for the daily GDI against the monthly SPI or SPEI (Table S1a) and the DAV for the monthly GDI against the monthly SPI or SPEI (Table S1b). The results obtained in Table S1a are identical to Table 2, where all locations reveal gains. Yet for Table S1b, some points have negative DAV. This behaviour hints at the fact that the added value of the index in this context is not only due to the comparison between a daily time step, with a monthly time step, but also to an overall better fit to the empirical distribution.

To evaluate the degree of similarity between the GDI against the other indices, the temporal correlation and the RMSE are presented in Fig. 3. Figures 3a and 3b show the comparison between the GDI against the corresponding SPI and SPEI, i.e., GDI (PR) is compared with SPI and GDI (PR-PET) compared to SPEI. The degree of agreement for most locations is very high, with correlations close to 1. The RMSE mirrors the results obtained for the correlations, with very low values, indicating a proximity of the index values across SPI or SPEI and the corresponding GDI. These outcomes suggest small differences amongst the indices across all timescales, i.e., GDI can detect the same drought events as SPI or SPEI. Fig. 3b displays the comparison between the GDI and the Z-Score, for both PR and the PR-PET as input. For Figure 3a, the correlations are still somewhat high with low RMSE, namely for the longer accumulations. A high correlation is still expected since the same time series were used for computing both the GDI and Z-Score. However, for the Z-Score, the prospect is different, which is expected since the underlying distribution of the raw data is non-normal (Fig. 2). Hence the larger differences found relative to the GDI. For the longer accumulations, the underlying distribution of the Z-Score data tends to be closer to the standard normal, resulting in lower RMSE values and an approximation between GDI and Z-Score. The dispersion of the values is also greater in comparison to Fig. 3a. For the 7-day accumulation, the correlation (RMSE) is approximately 0.9 (0.6), gradually increasing (decreasing) for longer accumulation periods.

Table 2. Distribution Added Value for (a) GDI against SPI or SPEI, (b) GDI against the Z-Score index. Each column denotes the accumulation periods, where PR stands for accumulated precipitation (left) and PR-PET stands for accumulated precipitation minus potential evapotranspiration (right). The colours and values in each cell correspond to the percentage of land points within the respective DAV category. The Perkins Skill Score is built by confronting each index histogram against the normal distribution histogram. The DAV is then computed as the relative difference between each index Perkins Skill Score, and for each location individually. The Table shows the percentage of land points falling within each DAV category.

a)

DAV %	PR							PR-PET						
	7D	15D	30D	90D	180D	360D	720D	7D	15D	30D	90D	180D	360D	720D
100														
95														
90														
85														
80														
75														
70														
65														
60														
55														
50														
45														
40														
35														
30	0.261	0.015												0.077
25	2.453	0.767	0.107				0.015							0.506
20	7.88	4.614	2.361	0.061		0.015	1.012						0.445	2.545
15	20.267	11.498	7.619	1.947	0.046	3.848	13.767					0.077	6.423	14.549
10	52.062	27.211	22.858	11.62	3.94	43.385	51.893	7.803	1.763	0.981	1.426	4.645	40.442	53.074
5	17.063	52.062	46.068	58.577	74.368	50.989	32.838	85.865	60.586	34.815	50.038	78.829	51.893	29.143
0	0.015	3.833	20.987	27.794	21.646	1.763	0.475	6.331	37.651	64.204	48.536	16.449	0.797	0.107
-5														
-10														
-15														

b)

DAV %	PR							PR-PET						
	7D	15D	30D	90D	180D	360D	720D	7D	15D	30D	90D	180D	360D	720D
100	0.138													
95	0.383													
90	0.981													
85	1.38													
80	1.564							0.368						
75	1.809							0.613						
70	2.284	0.092						0.659						0.015
65	4.201	0.169						0.583						0.077
60	7.772	0.69						1.334					0.061	0.23
55	11.283	1.932						2.024					0.215	0.23
50	20.221	2.591						5.396	0.644				0.337	0.184
45	19.5	3.081	0.153				0.015	9.014	1.15			0.031	0.123	0.169
40	14.84	9.627	1.272				0.107	19.991	1.61			0.337	0.092	0.184
35	9.03	20.911	4.047	0.092		0.061	0.337	31.013	4.706	0.261	0.061	0.245	0.107	0.337
30	4.201	29.618	11.452	1.518	0.245	0.445	0.69	21.202	15.499	2.637	0.399	0.245	0.138	1.042
25	0.399	19.654	32.04	5.488	1.303	1.38	3.863	7.144	29.296	6.132	0.69	0.184	0.491	3.219
20		10.287	29.005	24.943	8.784	10.164	17.492	0.521	33.803	29.833	3.664	1.472	4.446	13.583
15		1.349	20.788	39.966	35.858	41.039	44.841	0.138	12.648	44.887	30.216	17.4	31.78	47.723
10			1.242	27.503	48.659	44.136	32.117		0.613	15.744	58.225	71.087	59.375	32.776
5				0.491	5.151	2.775	0.537		0.031	0.506	6.745	8.999	2.836	0.23
0														
-5														
-10														
-15														

0 0.1 0.5 1 5 10 15 20 30 40 50 100

% of Land points

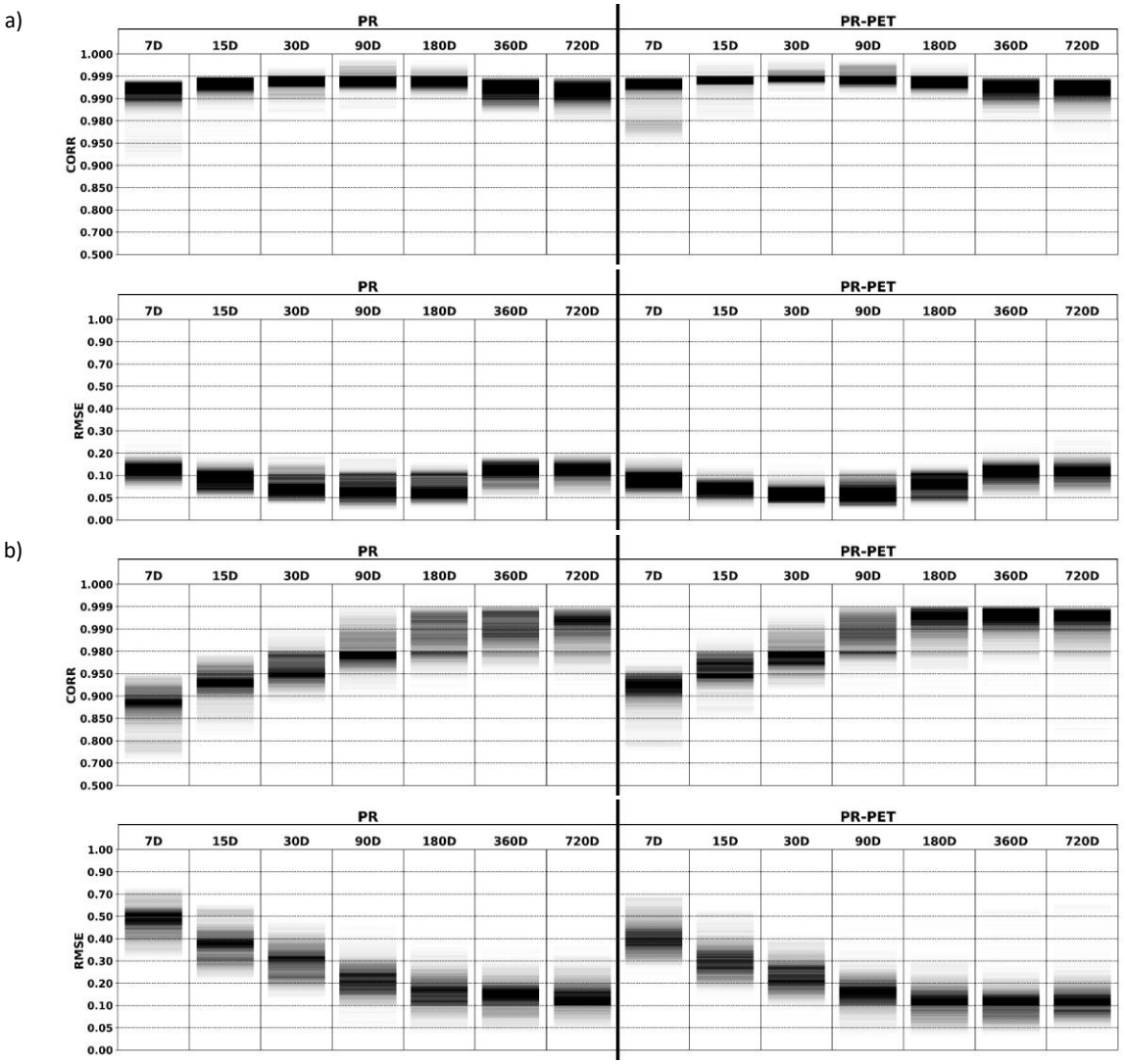

Figure 3. Pearson correlation and root Mean Squared Error between the GDI index against (a) SPI or SPEI, and (b) against the Z-score index. Each column denotes the accumulation periods, where PR stands for accumulated precipitation (left) and PR-PET stands for accumulated precipitation minus potential evapotranspiration (right). The lines depict individual land points for the IB01 observations, with darker shading indicating a higher density of closely spaced lines.

Figure S5 of the supplementary material shows the correlation and RMSE of the monthly GDI against the monthly SPI or SPEI. The findings are akin to those from Fig 3b, where the agreement between indices is higher for the longer accumulations.

3.2. Drought Characteristics Assessment

When evaluating the performance of a drought index, it is crucial to assess key characteristics such as event severity, frequency, duration and spatial extent. Table 3 presents the spatial correlation and RMSE for drought intensity, frequency, duration and spatial extent between the GDI against the SPI or SPEI (Table 3a) and against the Z-Score index (Table 3b). Only the results for moderate drought are considered since, for higher drought thresholds, the lack of events may hinder this comparison. Overall, the spatial agreement of the intensity and mean

duration of drought characteristics, between the GDI and SPI or SPEI (Table 3a) reduces towards the higher accumulations, as indicated by declining correlations and increasing RMSEs. Those results contrast with the findings from Figure 3, where correlations remained high and RMSE low for all timescales. As for the drought frequency, although the correlation decreases for higher aggregation periods, the RMSE also decreases. Nonetheless, for all cases and regardless of the accumulation time step, the higher the base values from each drought characteristic, shown in Fig. S6, S8 and S10, imply potentially larger differences amongst the indices. The spatial extent in drought reveals close values between the GDI and the SPI or SPEI, with near perfect correlation (near 1) and low RMSE values Comparing with the Z-Score index yields similar results to Table 3a, albeit with some differences, particularly at the 7-day accumulation for drought intensity and frequency. In this case, the correlations and RMSE do not follow the previous pattern. For instance, the correlation for drought intensity is 0.917 for the PR indices and 0.909 for the PR-PET indices, contrasting with 0.938 and 0.949 obtained in the same comparison of the GDI against the SPI or SPEI. Figures S7, S9 and S11, along with Table S2 show the same results for the monthly GDI and monthly SPI or SPEI indices. In this case, the comparability at shorter timescales is notably lower, particularly for PR indices, increasing towards higher accumulations.

Figure 4a displays the difference between GDI and SPI or SPEI for the drought characteristics mean event severity, decadal frequency, mean duration, and spatial extent for the three drought classes defined: moderate ($index < -0.5$), severe ($index < -1$) and extreme ($index < -1.5$). Regarding drought severity, the difference amongst indices increases for higher accumulations, with the GDI showing higher intensity for most locations, as indicated by the positive median value. In terms of drought decadal frequency, the differences vary more for all accumulations. At the 7-days accumulations, GDI tends to reveal less moderate and severe events, but more extreme events. Conversely, and for the PR based indices, at the 15-, 30- and 90-days, GDI slightly indicates more moderate events, while showing fewer severe and extreme events. The opposite occurs for the PR-PET based indices. It is important to note that the extreme drought class is contained within severe drought, which in turn is contained within moderate drought. This approach avoids splitting the events (Soares et al., 2023b). The position of the median in this context is relevant, indicating the trend shown by most locations. For the mean event duration not only does the dispersion of the results increase towards the longer accumulations, but the median value is also negative, suggesting systematic shorter events for the GDI index within the majority of locations. For severity and duration, the differences are higher for the longer accumulations, consistent with the findings in Table 3a, where greater variability for the differences implies lower correlation and higher RMSE. In opposition to the other drought characteristics, the spatial extent reveals fewer differences across all time scales, as anticipated from the results obtained in Table 3a. In this case, extreme drought tends to reveal lower differences than moderate and severe drought. It is worth noting that the scale is not linear thus, for higher values, the differences in the spread may not be as noticeable. Additionally, the inclusion of the PET does not change noticeably the results in this context.

Table 3. Spatial Pearson Correlation (blue) and spatial Root Mean Squared Error (red) between (a) GDI against SPI or SPEI and (b) GDI against the Z-Score index. Each row, for both panels and from top to bottom, represents the drought intensity, drought mean decadal frequency, and drought mean duration. The last row in both panels displays a time Pearson Correlation and Root Mean Squared Error for the drought spatial extent. These results are presented only for moderate drought (index< -0.5). Each column denotes the accumulation periods, where PR stands for accumulated precipitation (left) and PR-PET stands for accumulated precipitation minus potential evapotranspiration (right). The colours denote extremes of either correlation or RMSE.

a)

	PR							PR-PET						
	7D	15D	30D	90D	180D	360D	720D	7D	15D	30D	90D	180D	360D	720D
MES	0.938 / 0.387	0.984 / 0.258	0.972 / 0.426	0.890 / 0.685	0.916 / 1.282	0.734 / 3.210	0.757 / 4.655	0.949 / 0.298	0.985 / 0.210	0.983 / 0.313	0.939 / 0.752	0.881 / 1.555	0.737 / 3.294	0.717 / 4.698
MDF	0.965 / 5.062	0.977 / 3.324	0.961 / 3.102	0.870 / 2.672	0.882 / 1.487	0.901 / 1.419	0.895 / 1.380	0.976 / 4.560	0.978 / 2.425	0.962 / 1.956	0.935 / 1.501	0.915 / 1.449	0.881 / 1.522	0.869 / 1.424
MED	0.942 / 0.468	0.963 / 0.651	0.939 / 1.125	0.837 / 2.401	0.843 / 4.459	0.852 / 15.034	0.826 / 32.552	0.954 / 0.386	0.968 / 0.498	0.958 / 0.924	0.933 / 2.682	0.898 / 6.726	0.818 / 21.261	0.799 / 49.620
SPA	0.999 / 1.099	0.999 / 1.723	0.998 / 2.445	0.998 / 2.002	1.000 / 0.951	0.998 / 3.390	0.999 / 2.556	0.999 / 1.619	1.000 / 1.032	1.000 / 0.842	1.000 / 1.325	0.999 / 1.869	0.999 / 2.841	0.999 / 2.181

b)

	PR							PR-PET						
	7D	15D	30D	90D	180D	360D	720D	7D	15D	30D	90D	180D	360D	720D
MES	0.917 / 1.141	0.951 / 0.986	0.936 / 0.797	0.863 / 0.747	0.910 / 1.284	0.694 / 3.360	0.738 / 4.751	0.909 / 0.659	0.943 / 0.624	0.957 / 0.557	0.927 / 0.790	0.883 / 1.521	0.740 / 3.190	0.729 / 4.540
MDF	0.910 / 10.195	0.977 / 4.207	0.954 / 3.142	0.847 / 2.802	0.876 / 1.504	0.888 / 1.500	0.890 / 1.411	0.931 / 9.245	0.972 / 3.965	0.956 / 2.417	0.925 / 1.631	0.911 / 1.488	0.881 / 1.522	0.869 / 1.446
MED	0.923 / 0.617	0.932 / 0.874	0.905 / 1.316	0.799 / 2.753	0.821 / 4.954	0.833 / 16.657	0.810 / 34.399	0.942 / 0.606	0.946 / 0.910	0.939 / 1.344	0.917 / 3.076	0.893 / 6.920	0.824 / 20.398	0.743 / 54.505
SPA	0.998 / 2.765	0.998 / 2.096	0.998 / 1.792	0.998 / 1.811	1.000 / 1.323	0.997 / 4.092	0.999 / 2.755	0.996 / 4.377	0.998 / 3.381	0.999 / 2.327	0.999 / 1.834	0.999 / 1.943	0.999 / 2.467	1.000 / 1.510

Pearson Correlation: <0.7 >0.9

Root Mean Squared Error: <1 >10

Figure 4b illustrates the differences between the GDI and the Z-Score index. Since the Z-Score is a simple standardisation with no changes in the underlying distribution, one can anticipate larger differences, as suggested by the previous figures. Concerning mean drought severity, shorter accumulations of up to 30-days reveal that the GDI has fewer events than the Z-Score. For the higher accumulations, the differences tend to be more positive with more variability across all locations. Regarding drought decadal frequency, the same behaviour occurs for moderate drought. However, for severe and extreme drought, GDI reveals more events than the Z-Score, decreasing towards the longer accumulations. As for the mean drought duration, a similar behaviour can be observed, albeit with smaller differences in the shorter accumulations. Furthermore, and akin to the mean event severity, differences tend to be more spread out for longer accumulations. It is noteworthy that for severe and namely for extreme droughts, the Z-Score may show locations without events. The same may occur for GDI, SPI or SPEI, although with a lower chance. This clearly occurs for extreme drought, for instance atthe 7-day accumulation Z-Score index (Fig. S6, S8 and S10). Regarding drought spatial extent, GDI returns lower values for moderate drought and higher values for severe and extreme drought. The only exceptions are at the 360- and 720-days accumulations, where most locations reveal a slightly negative difference. Overall, the results in Fig. 4 do not indicate a significant alteration between the PR and PR-PET based indices, consistent with the findings in Fig. 3 for the correlation and RMSE of the time series, as well as Table 3.

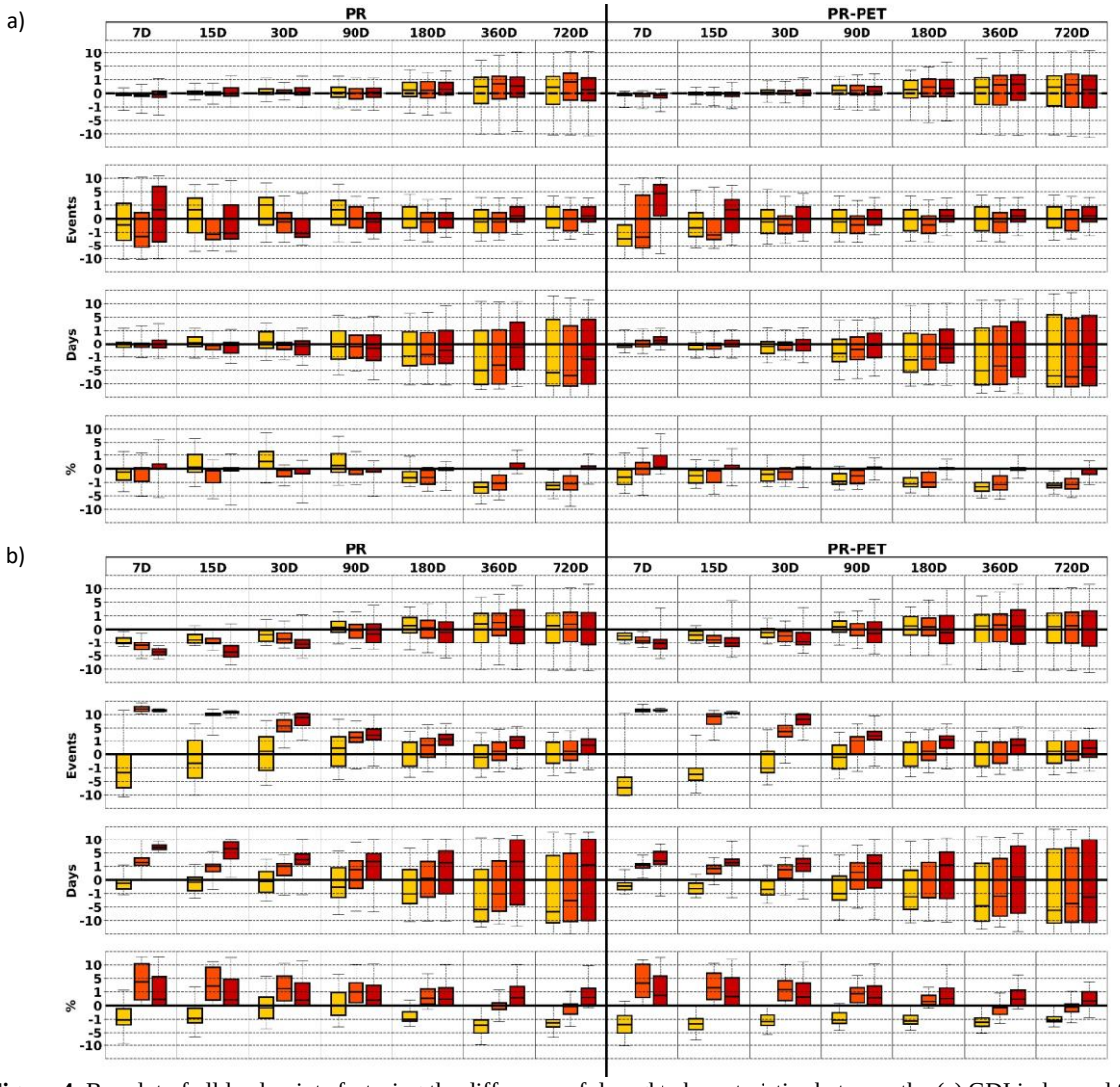

Figure 4. Boxplot of all land points featuring the difference of drought characteristics between the (a) GDI index and SPI or SPEI and between (b) GDI index and Z-Score index. In each sub-figure, from top to bottom: the mean event severity, decadal frequency, mean event duration and spatial extent of droughts. For the case of drought spatial extent, the differences are made for each time step. Each column denotes the accumulation periods, where PR stands for accumulated precipitation (left) and PR-PET stands for accumulated precipitation minus potential evapotranspiration (right). The different boxplot denotes the results for moderate drought for index <-0.5 (yellow), severe drought for index <-1 (orange) and extreme drought for index <-1.5 (red). For each boxplot, the low (high) whisker denotes the 1st (99th) percentile, while the three horizontal lines within the box correspond, from bottom to top to the 25th, 50th and 75^{t} percentiles.

It appears that the variations between the PR and PR-PET indices are more evident within the indices themselves rather than in the comparisons performed amongst them. Figure S12 shows the same differences but for the monthly GDI against the monthly SPI or SPEI.

3.3. 2004/2005 Case Study

A case study of an extreme drought which affected the Iberian Peninsula, starting in the autumn of 2004 is presented in Fig. 5, where the spatial extent for moderate, severe, and extreme drought are shown, computed for

all timescales and indices. Figure S13 in the supplementary material shows the same but for the PR-based indices. The differences between the PR and PR-PET based indices is minimal in terms of drought spatial extent, as expected from the previous results. The 2005 drought is widely regarded as one of the most extreme events in recent history affecting the Iberian Peninsula, characterised by a precipitation deficit during the hydrological year of 2004/2005 (García-Herrera et al., 2007; Santos et al., 2007). The patterns of the spatial extent for all drought severities for the lower accumulations (Figs. 5a, 5b and 5c) are similar, revealing the extremely dry autumn of 2004 and spring of 2005, which somewhat repeated in the following hydrological year. At these scales, the GDI, SPI and SPEI indices exhibit similar percentages of territory in the three drought categories.

The SPEI and GDI show that over 75% of the land experienced extreme drought conditions from October 2004 to May 2005. Conversely, the Z-Score stands out with lower spatial percentages of Iberia experiencing severe drought and almost no territory is classified as extreme drought. As for the longer accumulations (Figs. 5d to 5g), all three indices converge regarding the spatial extent of drought. At 90- and 180-days accumulation almost the entire year of 2005 was at least in moderate drought, returning to normal conditions in 2006. For the 360-day accumulation, the peak of drought severity occurs during the summer and autumn of 2005. It is worth noting that summer is typically one of the most critical periods for drought due to reduced precipitation and increased temperatures. For the 720 days, however, the drought conditions started in 2005 with a peak in 2006, revealing a shift relative to the previous cases due to the longer accumulation. As indicated by the results from Figs. 5a to 5c, the autumn of 2005 and spring of 2006 were also drier, albeit not as severe as during the previous hydrological year.

Figure 6 shows the time series of the spatial means of the PR-PET indices for the same period and event as Fig. 5 (October 2004 to September 2006). Figure S14 shows the same, but for the PR based indices. The red and blue shadings denote the differences between the GDI (solid black line) the SPEI and the Z-Score, respectively. Amongst all aggregation periods (Figs. 6a to 6g), the differences across indices are more visible towards the extreme values. Overall, the differences are larger for the Z-Score rather than for the SPEI. Since the Z-Score is based on a simple standardisation, it closely follows the accumulated PR-PET patterns, while the same does not occur for the other indices, hence the higher differences. Still, for the lower aggregation periods (Figs. 6a to 6c), the Z-Score fluctuates more relative to the SPEI and GDI. As for the GDI, the day-to-day values can reach higher extremes. Since the index is based on an empirical distribution, the maximum and minimum of the time series is dependent on the length of the data used. On the other hand, for indices such as the SPEI, the extremes are more controlled by the chosen distribution, while for the Z-Score, the extremes are dependent on the difference of the accumulations relative to their mean. Those factors may cause a smoothing effect on the extremes for the SPEI, SPI and Z-Score.

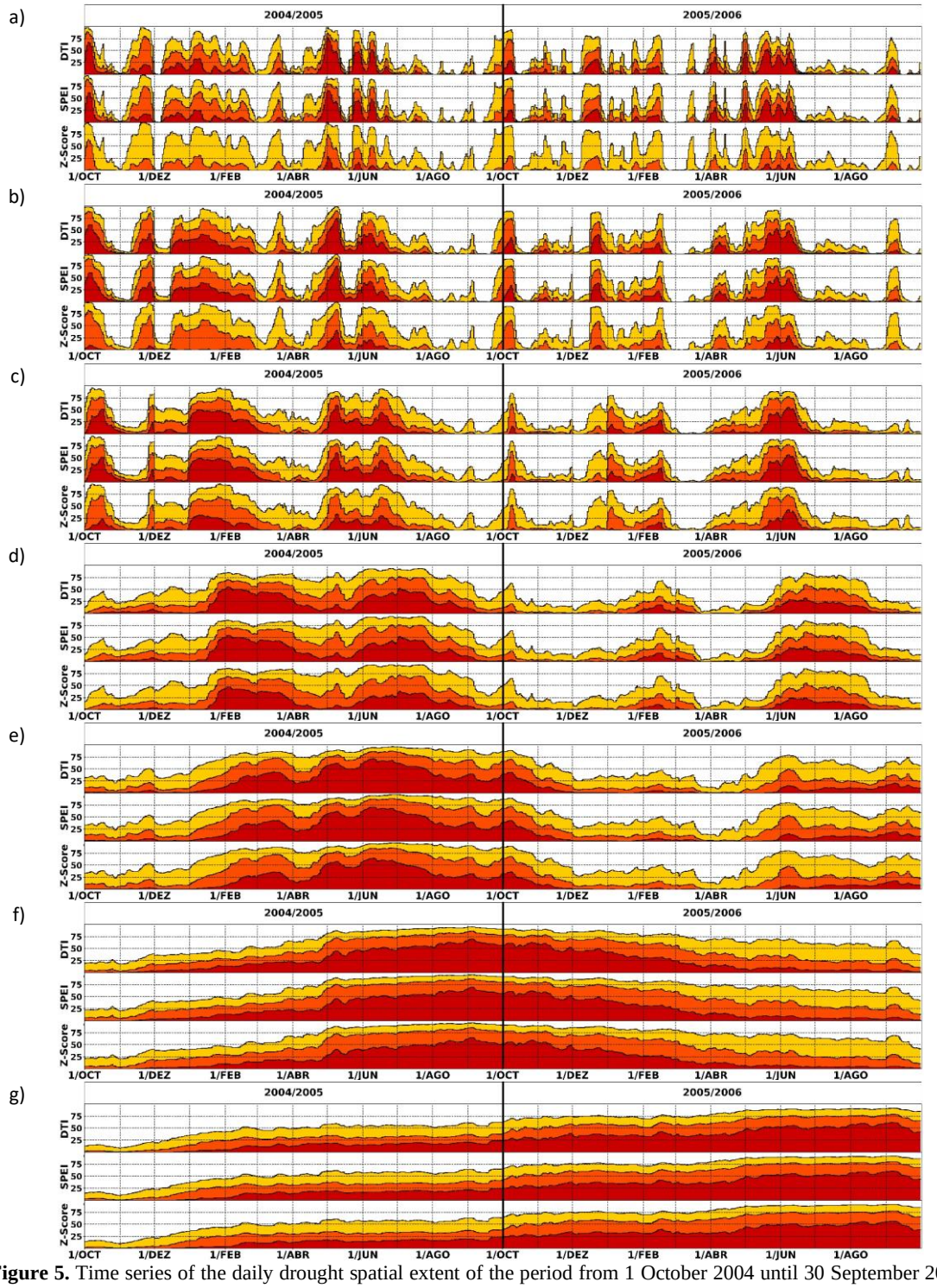

Figure 5. Time series of the daily drought spatial extent of the period from 1 October 2004 until 30 September 2006 for the IB01 with aggregations of (a) 7-, (b) 15-, (c) 30-, (d) 90-, (e) 180-, (f) 360- and (g) 720-days. In each panel, the top row displays the results for the GDI index, the middle row for the SPEI index and the bottom row for the Z-Score standardisation. All indices consider only the balance between precipitation and PET. The yellow colour denotes the results for moderate drought for index <-0.5, light orange for severe drought for index <-1 and dark orange for extreme drought for index <-1.5.

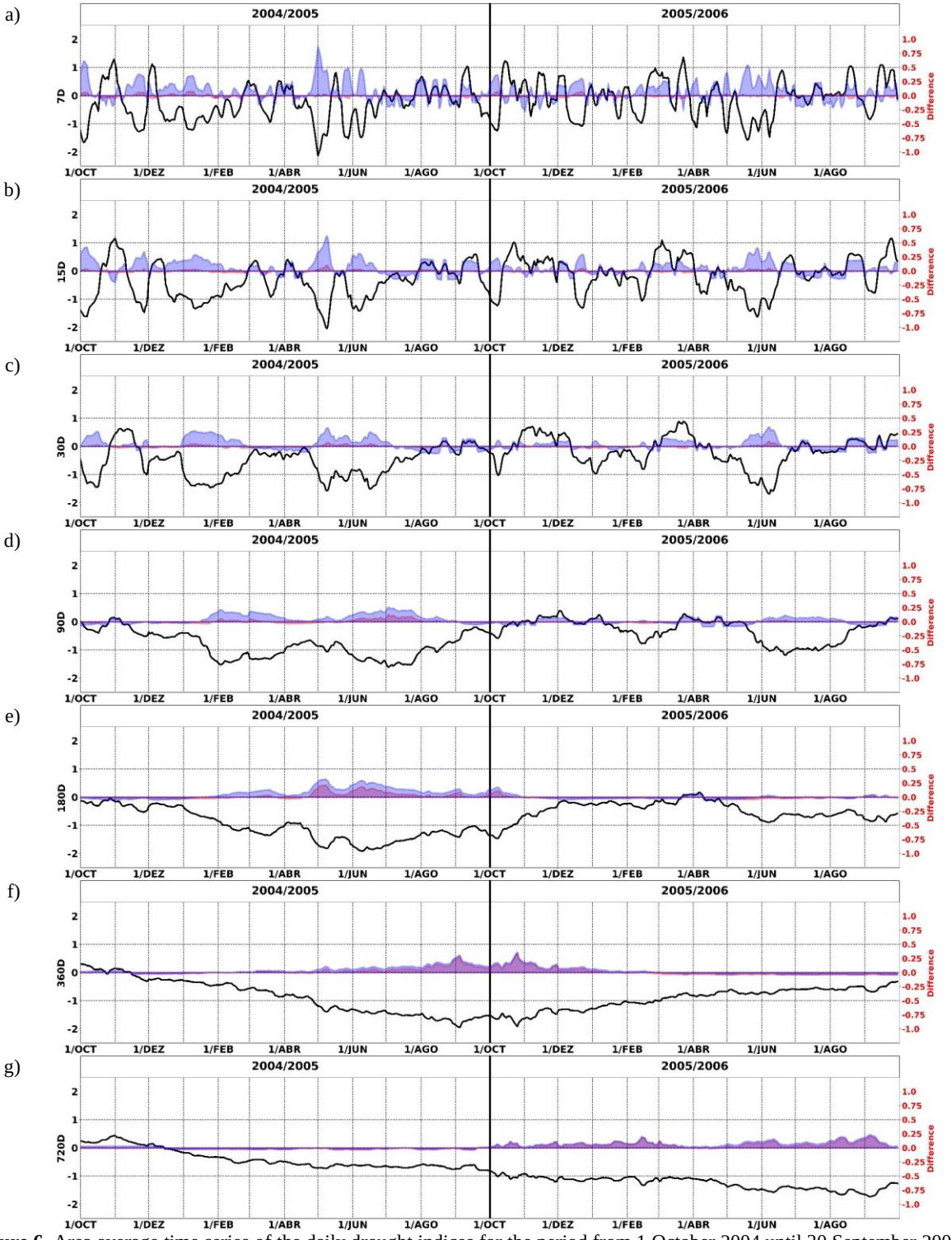

Figure 6. Area average time series of the daily drought indices for the period from 1 October 2004 until 30 September 2006 for the IB01 dataset with aggregations of (a) 7-, (b) 15-, (c) 30-, (d) 90-, (e) 180-, (f) 360- and (g) 720-days. The black line represents the GDI index, while the red and blue shadings denote, respectively, differences between the GDI and SPEI and between GDI and the Z-Score index. The differences are computed by taking the absolute value of each index first. Thus, if the difference is positive, it implies that the GDI is further away from the mean 0 than the other index. All indices only consider the balance between precipitation and PET.

4. Discussion and Conclusions

In the present chapter, a new drought index is introduced, designated as Generalised Drought Index or GDI. This index is extremely straightforward to compute since the fitting process to a known distribution is not required. It is empirically driven and can be regarded as an alternative to other indices such as SPI or SPEI. The GDI is computed by generating an empirical distribution based on a smoothed cumulative histogram, where the PR or PR-PET data can be converted into probabilities and then brought back as standardised values following a normal distribution of mean 0 and a standard deviation of 1. As an example, the IB01 observational-based dataset was used to compute the GDI for Iberia. The analysis considers the IB01 period from 1971 to 2015. To compare and to assess the proposed index added value, the daily SPI, SPEI and Z-Score indices were computed with a daily time step, for PR and PR-PET based accumulations. A comparison with the monthly SPI and SPEI is also performed and shown in the supplementary material.

The main distinction between GDI and SPI or SPEI lies in the fitting of climate data to a probability distribution function. In the case of the monthly SPI and SPEI, the fitting process is mandatory due to the scarcity of data points compared to daily data, which hinders the applicability of the GDI. Nonetheless, in this study, and since the seasonal cycle was previously removed, both the daily SPI and SPEI were fitted to the log-logistic distributions. The reason to consider the log-logistic distribution for SPI lies in the poor fit found for the Gamma distribution. It is important to note that assuming a specific distribution for different climate types or even different accumulations can be detrimental since the underlying distributions may differ (e.g., Stagge et al., 2015; Monish and Rehana, 2020; Zhang and Li 2020) as also shown in Fig S1. Those issues do not arise with the GDI index. Furthermore, SPI and SPEI may encounter difficulties in fitting data from semi-arid and arid climates with very low accumulations, such as deserts (Beguería et al., 2014). The very low accumulations, which could also occur in climate change studies with historical reference, may not be very well simulated, although alternative approaches exist, such as Spinoni et al. (2018) and Soares et al. (2023a). On the other hand, the GDI does not have those constraints since the distribution is built empirically by smoothing an accumulated data histogram. Apart from the distribution, the definition of the parameters in the case of SPI and SPEI may also pose challenges, especially at the daily scale. Outliers present in the data may hinder the parameter estimation process. Additionally, as the dataset size increases, the computational expense for calculating the index also escalates, particularly when considering methods such as maximum likelihood (Beguería et al., 2014). In contrast, the GDI offers a simple and computationally efficient procedure which easily bypasses the determination of fitting parameters, making it suitable for large datasets. The performance of the GDI may be superior for larger datasets, as the underlying distribution associated with each location is better defined. Indeed, the GDI time series conforms better to the theoretical standard normal distribution, namely if PET is considered. Another potential source of uncertainty, particularly for extreme values, is associated with the Abramowitz and Stegun (1965) approximation, which performs better for values closer to the mean. For extremes, the values deviate from the true standard normal distribution, although the likelihood of SPI or SPEI being extreme is low (Stagge et al., 2015). GDI does not exhibit this limitation due to its empirical nature; the minimum and maximum values of the index are dependent on the size of the time series and these values do not deviate from the standard normal as much as the

other indices.

Regarding the evaluation of the proposed metric with a version of the DAV, using the normal distribution as a reference, the GDI exhibits a positive added value against the other drought indices. The gains of the proposed index against the SPI and SPEI are relevant since both indices already conform to the standard normal distribution. Those findings could potentially indicate a reduction of the uncertainty due to the fitting procedures. Thus, this added value is not solely owned to the different standardisation methodologies, otherwise the DAV would be closer to 0 % in this case. As for the comparison against the Z-Score, the GDI displays higher DAV percentages as expected, highlighting the relevance of the underlying distribution in thresholds based on standard deviations from the mean, such as those used in GDI, SPI or SPEI.

To assess the degree of similarity amongst the indices, a Pearson correlation and a RMSE were computed. The results reveal a strong agreement amongst the three indices, particularly between the GDI with SPI or SPEI. Nevertheless, lower correlations and higher RMSE occur for the comparison to the Z-Score. In this case, those deviations are expected since the original underlying distribution is kept. Regarding the drought characteristics such as intensity, frequency, and duration, for moderate drought conditions, the GDI shows similar results against the SPI, SPEI and Z-Score. Still, the proposed index reveals differences since, for most cases and towards longer aggregation periods, the similarity amongst indices decreases.

The GDI is also evaluated in terms of drought spatial extent against the SPEI and Z-Score for the severe 2004/2005 drought event. While GDI, SPI and SPEI reveal very similar values for all timescales and drought severities, the Z-Score had some difficulty in representing severe and namely extreme drought for the lower accumulations. All indices tend to converge due to the approximation towards normality for longer accumulations. Regarding the performance of the GDI, the proposed index demonstrated a close representation of the spatial extent of drought compared to SPEI. The same conclusions can be drawn for the PR-based indices. As for the spatial mean time series the indices tend to grow apart towards the extreme values. Nevertheless, the differences are small, particularly for the comparison of GDI against the SPI or SPEI. Those findings provide reassurance and present the GDI as a viable alternative to the SPI or SPEI indices.

The Z-Score synchronises only the statistical mean and standard deviation by setting them to 0 and 1, respectively, disregarding the underlying distribution. In contrast, GDI, SPI or SPEI share the same distribution and parameters: the standard normal distribution with a mean of 0 and a standard deviation of 1. PR or even PR-PET tend to be positively skewed, which may result in an underrepresentation of severe and extreme drought for shorter accumulations on threshold-based definitions. Since GDI, SPI or SPEI indices, follow the standard normal distribution, this issue does not arise. If a percentile-based threshold were used, differences in decadal drought frequency, mean event duration, and spatial extent would likely be reduced. However, using a threshold based on percentiles could hinder the comparison amongst indices, as the intensity of individual events and the index value for each day would vary.

The GDI index can identify the same events as SPI or SPEI by returning similar results for most cases while revealing an enhanced performance. However, it is less computationally expensive, does not need the assumption of the characteristics of the underlying distribution of the data and can be applied to other variables such as soil

moisture or actual evapotranspiration. Comparatively to other studies also featuring a daily drought index (e.g., Li et al., 2020; Ma et al., 2020, Zhang et al., 2022a), the daily approach to GDI offers a finer temporal resolution, enabling a more detailed depiction of meteorological variations and their immediate impacts on drought conditions. The higher sensitivity compared to monthly indices allows for the timely identification of short-term drought events, better capturing the start and duration. This feature is particularly relevant in regions characterised by a sizeable climatic variability. Thus, GDI is suitable for describing meteorological, hydrological, agricultural and flash droughts using the same methodology. Therefore, GDI could be a viable alternative for computing a standardised index for drought analysis and simulation evaluation with EURO-CORDEX simulations or the large kilometre-scale simulations from the WRCP Flagship Pilot Study on "Convective phenomena over Europe and the Mediterranean". The assessment of simulations with a daily drought index allows researchers to scrutinise models more rigorously, examining not just their ability to predict long-term trends but also their effectiveness in capturing short-term variability. With the use of a daily drought index, the assessment of a model's performance regarding frequency, severity and duration of events is thus enhanced. Furthermore, the daily index enhances our understanding of the feedback mechanisms between meteorological droughts and their impacts on sectors such as agriculture and water management. Unlike traditional indices, which might aggregate data over longer periods and potentially smooth out critical variations, the daily index preserves the day-to-day variations in moisture availability. This is crucial for understanding drought onset, evolution and dissipation, as well as for predicting their impact on crop yields, water supply, and other critical resources. As climate simulations evolves, daily drought indices will undoubtedly play a key role in ensuring that the same models are able to meet the challenges posed by a rapidly changing climate.

Nevertheless, some questions are still open. Firstly, how different are the GDI results for climate change projections? The proposed index is empirically based; thus, the approach from Spinoni et al. (2018) or Soares et al. (2023a) can be considered for climate change assessment, where the entire time series is considered to build the empirical distribution. However, it would still be possible to use the historical period as a reference, conserving the absolute values for both the reference and future periods? What is the applicability and performance of the index at a global level? Other questions also arise, namely the sensitivity of the index to the potential evapotranspiration method considered and the sensitivity related to the initial variables. Furthermore, can the index be used for an ensemble-based analysis? Some of these questions will be pursued in future studies.

Data availability.

All model and observational datasets are publicly available. The regional and global model data are available through the Earth System Grid Federation portal (Williams et al., 2011; https://esgf.llnl.gov/, last access: September 2023). The Iberia01 dataset is publicly available through the DIGITAL.CSIC open science service (Herrera et al., 2019a, https://doi.org/10.20350/digitalCSIC/8641).

Author contributions

João Careto developed the new drought metric the GDI, designed and wrote the paper. Rita Cardoso, Ana Russo, Daniela Lima and Pedro Soares provided useful insights and made major contributions to the writing process. All authors read and approved the final manuscript.

Competing interests.

The contact author has declared that neither they nor their co-authors have any competing interests.

Acknowledgements

The authors would like to acknowledge the Iberian Gridded Dataset (IB01) http://hdl.handle.net/10261/183071 (Last access: 12 December 2023). The authors also wish to acknowledge the Institute Dom Luiz, the Faculty of Sciences from the University of Lisbon, the Portuguese Foundation for Science and Technology and also the Copernicus Climate Change Service (C3S, https://climate.copernicus.eu/).

Funding

This work was supported by the Portuguese Fundação para a Ciência e a Tecnologia (FCT) I.P./MCTES through national funds (PIDDAC) – UIDB/50019/2020 (https://doi.org/10.54499/UIDB/50019/2020), UIDP/50019/2020 (https://doi.org/10.54499/UIDP/50019/2020), DHEFEUS (https://doi.org/10.54499/2022.09185.PTDC). JAMC, RMC, AR and DCAL are supported by the Portuguese Foundation for Science and Technology (FCT) financed by national funds from the MCTES through grants SFRH/BD/139227/2018, https://doi.org/10.54499/2022.01167.CEECIND/CP1722/CT0006 and https://doi.org/10.54499/2022.03183.CEECIND/CP1715/CT0004, respectively.

References

Abramowitz, M. and Stegun, I. A.: Handbook of Mathematical Functions, Dover Publications, New York, 1965.

Ahmad, M. I., Sinclair, C. D., and Werritty, A.: Log-logistic flood frequency analysis. Journal of Hydrology, 98(3-4), 205-224, doi:10.1016/0022-1694(88)90015-7, 1988.

Akhtari, R., Morid, S., Mahdian, M. H., and Smakhtin, V.: Assessment of areal interpolation methods for spatial analysis of SPI and EDI drought indices, International Journal of Climatology: A Journal of the Royal Meteorological Society, 29(1), 135-145, doi:10.1002/joc.1691, 2009.

Allen RG, Pereira LS, Raes D, Smith M.: FAO Irrigation and drainage paper No 56 Rome: Food and Agriculture Organisation of the United Nations 56 156, 1998. http://www.climasouth.eu/sites/default/files/FAO%2056.pdf (Last accessed 29th July 2023)

Alley, W. M.: The Palmer drought severity index: limitations and assumptions, Journal of Applied Meteorology and Climatology, 23(7), 1100-1109, doi:10.1175/1520-0450(1984)023<1100:TPDSIL>2.0.CO;2, 1984.

Ban, N., Caillaud, C., Coppola, E., Pichelli, E., Sobolowski, S., Adinolfi, M., Ahrens, B., Alias, A., Anders, I., Bastin, S., Belušić, D., Berthou, S., Brisson, E., Cardoso, R. M., Chan, S. C., Christensen, O. B., Fernández, J., Fita, L., Frisius, T., Gašparac, G., Giorgi, F., Goergen, K., Haugen, J, E., Hodnebrog, Ø., Kartsios, S., Katragkou, E., Kendon, E. J., Keuler, K., Lavin-Gullon, A., Lenderink, G., Leutwyler, D., Lorenz, T., Maraun, D., Mercogliano, P., Milovac, J., Panitz, H. J., Raffa, M, Remedio, A. R., Schär, C., Soares, P. M. M., Srnec, L., Steensen, B. MM., Stocchi, Tölle, Truhetz, Temprado, J. V., de Vries, H., Warrach.-Sagi, K., Wulfmeyer, V. and Zander, M. J. The first multi-model ensemble of regional climate simulations at kilometer-scale resolution, part I: evaluation of precipitation. Climate Dynamics, 57, 275-302, doi: 10.1007/S00382-021-05708-W, 2021.

Beguería, S., Vicente-Serrano, S. M., Reig, F., and Latorre, B.: Standardised precipitation evapotranspiration index (SPEI) revisited: parameter fitting, evapotranspiration models, tools, datasets and drought monitoring, International journal of climatology, 34(10), 3001-3023, doi:10.1002/joc.3887, 2014.

Cardoso, R. M., Soares, P. M., Lima, D. C., and Miranda, P. M.: Mean and extreme temperatures in a warming climate: EURO CORDEX and WRF regional climate high-resolution projections for Portugal, Climate Dynamics, 52, 129-157, doi:10.1007/s00382-018-4124-4 , 2019

Cardoso, R. M., and Soares, P. M.: Is there added value in the EURO-CORDEX hindcast temperature simulations? Assessing the added value using climate distributions in Europe, International Journal of Climatology, 42(7), 4024-4039, doi:10.1002/joc.7472, 2022.

Careto, J. A. M., Soares, P. M. M., Cardoso, R. M., Herrera, S., and Gutiérrez, J. M.: Added value of EURO-CORDEX high-resolution downscaling over the Iberian Peninsula revisited–Part 1: Precipitation. Geoscientific Model Development, 15(6), 2635-2652, doi:10.5194/gmd-15-2635-2022, 2022a.

Careto, J. A. M., Soares, P. M. M., Cardoso, R. M., Herrera, S., and Gutiérrez, J. M.: Added value of EURO-CORDEX high-resolution downscaling over the Iberian Peninsula revisited–Part 2: Max and min temperature, Geoscientific Model Development, 15(6), 2653-2671, doi:10.5194/gmd-15-2653-2022, 2022b.

Carvalho, D., Cardoso Pereira, S., and Rocha, A.: Future surface temperature changes for the Iberian Peninsula according to EURO-CORDEX climate projections, Climate Dynamics, 56, 123-138, doi:10.1007/s00382-020-05472-3, 2021.

Casanueva, A., Kotlarski, S., Herrera, S., Fernández, J., Gutiérrez, J. M., Boberg, F., Colette, A., Christensen, O. B., Goergen, K., Jacob, D., Keuler, K., Nikulin, G., Teichmann, C., and Vautard, R.: Daily precipitation statistics in a EURO-CORDEX RCM ensemble: added value of raw and bias-corrected high-resolution simulations, Climate Dynamics, 47, 719-737, doi:10.1007/s00382-015-2865-x, 2016a.

Casanueva, A., Herrera, S., Fernández, J., and Gutiérrez, J. M.: Towards a fair comparison of statistical and dynamical downscaling in the framework of the EURO-CORDEX initiative, Climatic Change, 137, 411-426, doi:10.1007/s10584-016-1683-4, 2016b.

Chen, M., Shi, W., Xie, P., Silva, V.B., Kousky, V.E., Wayne Higgins, R. and Janowiak, J.E.: Assessing objective techniques for gauge-based analyses of global daily precipitation. Journal of Geophysical Research: Atmospheres, 113(D4).10.1029/2007JD009132, 2008.

Christian, J. I., Martin, E. R., Basara, J. B., Furtado, J. C., Otkin, J. A., Lowman, L. E., Hunt, E. D., Mishra, V. and Xiao, X.: Global projections of flash drought show increased risk in a warming climate. Communications Earth and Environment, 4(1), 165, doi: s43247-023-00826-1, 2023.

Coppola, E., Sobolowski, S., Pichelli, E., Raffaele, F., Ahrens, B., Anders, I., Ban, N., Bastin, S., Belda, M., Belusic, D., Caldas-Alvarez, A., Cardoso, R. M., Davolio, S., Dobler, A., Fernadez, J., Fita, L., Fumiere, Q., Giorgi, G., Goergen, K., Güttler, I., Halenka, T., Heinzeller, D., Hodnebrog, Ø., Jacob, D., Kartsios, S., Katragkou, E., Kendon, E., Khodayar, S., Kunstmann, H., Knist, S., Lavín-Gullón, A., Lind, P., Lorenz, T., Maraun, D., Marelle, L., van Meijgaard, E., Milovac, J., Myhre, G., Panitz, H-J., Piazza, M., Raffa, M., Raub, T, Rockel, B., Schär, C., Sieck., Soares, P. M. M., Somot, S., Srnec, L., Stocchi, P., Tölle, M. H., Truhertz, Vautard, R., de Vries, H., and Warrach-Sagi, K. A first-of-its-kind multi-model convection permitting ensemble for investigating convective phenomena over Europe and the Mediterranean. Climate Dynamics, 55, 3-34, doi: 10.1007/s00382-018-4521-8, 2020.

Cornes, R.C., van der Schrier, G., van den Besselaar, E.J. and Jones, P.D.: An ensemble version of the E-OBS temperature and precipitation data sets. Journal of Geophysical Research: Atmospheres, 123, 9391-9409, doi:10.1029/2017JD028200, 2018.

Dai, A.: Drought under global warming: a review, Wiley Interdisciplinary Reviews: Climate Change, 2(1), 45-65, doi:10.1002/wcc.81, 2011.

Dee, D. P., Uppala, S. M., Simmons, A. J., Berrisford, P., Poli, P., Kobayashi, S., Andrae, U., Balmaseda, M. A., Bauer, P., Bechtold, P., Beljiaars, A. C. M., van de Berg, L., Bidlot, J., Bormann, N., Delsol, C., Dragani, R., Fuentes, M., Geer, A. J., Haimberger, L., Healy, S. B., Hersbach, H., Hólm, E. V., Isaksen, L., Kållberg, P., Köhler, M., Matricardi, M., McNally, A. P., Monge-Sanz, B. M., Morcrette, J. -J., Park, B, -K., Peubey, C., de Rosnay, P., Tavolato, C., Thépaut, J, -N., and Vitart, F.: The ERA-Interim reanalysis: Configuration and performance of the data assimilation system, Quarterly Journal of the royal meteorological society, 137(656), 553-597, doi:10.1002/qj.828, 2011.

Droogers, P., and Allen, R. G.: Estimating reference evapotranspiration under inaccurate data conditions. Irrigation and drainage systems, 16, 33-45, doi:10.1023/A:1015508322413, 2002.

Edwards, D. C.: Characteristics of 20th Century drought in the United States at multiple timescales, Air Force Inst of Tech Wright-Patterson Afb Oh. 1997. https://apps.dtic.mil/sti/pdfs/ADA325595.pdf (Last accessed on 16th October 2023)

Farmer, W., Strzepek, K., Schlosser, C. A., Droogers, P., and Gao, X.: A method for calculating reference evapotranspiration on daily timescales, MIT Joint Program on the Science and Policy of Global Change, 2011. https://dspace.mit.edu/bitstream/handle/1721.1/61773/MITJPSPGC_Rpt195.pdf?sequence=1&isAllowed=y (Last accessed on 16th October 2023).

Fonseca, D., Carvalho, M. J., Marta-Almeida, M., Melo-Gonçalves, P., and Rocha, A.: Recent trends of extreme temperature indices for the Iberian Peninsula. Physics and Chemistry of the Earth, Parts A/B/C, 94, 66-76, doi:10.1016/j.pce.2015.12.005, 2016.

Fritsch, F. N., and Butland, J.: A method for constructing local monotone piecewise cubic interpolants. SIAM journal on scientific and statistical computing, 5, 300-304, doi:10.1137/0905021, 1984.

García-Herrera, R., Hernández, E., Barriopedro, D., Paredes, D., Trigo, R. M., Trigo, I. F., and Mendes, M. A.: The outstanding 2004/05 drought in the Iberian Peninsula: associated atmospheric circulation. Journal of Hydrometeorology, 8(3), 483-498, doi:10.1175/JHM578.1, 2007.

Gelaro, R., McCarty, W., Suárez, M.J., Todling, R., Molod, A., Takacs, L., Randles, C.A., Darmenov, A., Bosilovich, M.G., Reichle, R. and Wargan, K.: The modern-era retrospective analysis for research and applications, version 2 (MERRA-2). Journal of climate, 30, 5419-5454, doi:10.1175/JCLI-D-16-0758.1, 2017.

Giorgi, F., Jones, C., and Asrar, G. R.: Addressing climate information needs at the regional level: the CORDEX framework, World Meteorological Organisation (WMO) Bulletin, 58(3), 175, 2009. http://wcrp.ipsl.jussieu.fr/cordex/documents/CORDEX_giorgi_WMO.pdf (Last accessed on 29th July 2023)

Gutowski Jr, W. J., Giorgi, F., Timbal, B., Frigon, A., Jacob, D., Kang, H. S., Raghavan, R., Lee, B., Lennard, C., Nikulin, G., O'Rourke, E., Rixen, M., Solman, S., Stephenson, T., and Tangang, F.: WCRP coordinated regional downscaling experiment (CORDEX): a diagnostic MIP for CMIP6, doi:10.5194/gmd-9-4087-2016, 2016.

Guttman, N. B.: Comparing the palmer drought index and the Standardised precipitation index 1. JAWRA Journal of the American Water Resources Association, 34(1), 113-121, doi:10.1111/j.1752-1688.1998.tb05964.x, 1998

Guttman, N. B.: Accepting the Standardised precipitation index: a calculation algorithm 1. JAWRA Journal of the American Water Resources Association, 35(2), 311-322, doi:10.1111/j.1752-1688.1999.tb03592.x, 1999.

Hayes, M. J., Svoboda, M. D., Wiihite, D. A., and Vanyarkho, O. V.: Monitoring the 1996 drought using the Standardised precipitation index. Bulletin of the American meteorological society, 80(3), 429-438, doi:10.1175/1520-0477(1999)080<0429:MTDUTS>2.0.CO;2, 1999.

Hersbach, H., Bell, B., Berrisford, P., Hirahara, S., Horányi, A., Muñoz-Sabater, J., Nicolas, J., Peubey, C., Radu, R., Schepers, D. and Simmons, A.: The ERA5 global reanalysis. Quarterly Journal of the Royal Meteorological Society, 146, 1999-2049, doi: 10.1002/qj.3803, 2020.

Hersbach, H., Bell, B., Berrisford, P., Biavati, G., Horányi, A., Muñoz Sabater, J., Nicolas, J., Peubey, C., Radu, R., Rozum, I., Schepers, D., Simmons, A., Soci, C., Dee, D., Thépaut, J-N.: ERA5 hourly data on single levels from 1940 to present. Copernicus Climate Change Service (C3S) Climate Data Store (CDS), doi:10.24381/cds.adbb2d47, 2022.

Herrera, S., Cardoso, R. M., Soares, P. M., Espírito-Santo, F., Viterbo, P., and Gutiérrez, J. M.: IB01: A new gridded dataset of daily precipitation and temperatures over Iberia. Earth System Science Data, 11(4), 1947-1956, doi:10.5194/essd-11-1947-2019, 2019.

Herrera, S., Soares, P. M., Cardoso, R. M., and Gutiérrez, J. M.: Evaluation of the EURO-CORDEX regional climate models over the Iberian Peninsula: Observational uncertainty analysis. Journal of Geophysical Research: Atmospheres, 125(12), e2020JD032880, doi:10.1029/2020JD032880, 2020.

Hu, Q., and G. D. Willson.: Effect of temperature anomalies on the Palmer drought severity index in the central United States, International Journal of Climatology., 20, 1899–1911, doi:10.1002/1097-0088(200012)20:15<1899::AID-JOC588>3.0.CO;2-M, 2000.

Hunt E D, Svoboda M, Wardlow B, Hubbard K, Hayes M, Arkebauer T.: Monitoring the effects of rapid onset of drought on non-irrigated maise with agronomic data and climate-based drought indices, Agriculture and Forest Meteorology, 191: 1–11, doi:10.1016/j.agrformet.2014.02.001, 2014.

Jacob, D., Petersen, J., Eggert, B., Alias, A., Christensen, O. B., Bouwer, L. M., Braun, A., Colettem A., Déqué, M., Georgievski, G., Georgopoulou, E., Gobiet, A., Menit, L., Nikulin, G., Haensler, A., Hempelmann, N., Jones, C., Keuler, K., Kovats, S., Kröner N., Kotlarski, S., Kriiegsmann, A., Martin, E., van Mejigaard, E., Moseley, C., Pfeifer, S., Preuschmann, S., Radermacher, C., Radtke, K, Rechid, D., Rounsevell, M., Samuelsson, P., Somot, S., Soussana, J-F., Teichmann, C., Valentini, R., Vautard, R., Weber, B., and Yiou, P.: EURO-CORDEX: new high-resolution climate change projections for European impact research, Regional environmental change, 14, 563-578, doi:10.1007/s10113-013-0499-2, 2014.

Jacob, D., Teichmann, C., Sobolowski, S., Katragkou, E., Anders, I., Belda, M., Benestad, R., Boberg, F., Buonomo, E., Cardoso, R. M., Casanueva, A., Christensen, O. B., Christensen, J. H., Coppola, E., De Cruz, L., Davin, E. L., Dobler, A., Domínguez, M., Fealy, R., Fernandez, J., Gaertner, M. A., García-Díez, M., Giorgi, F., Gobiet, A., Goergen, K., Gómez-Navarro, J. J., Alemán, J. J. G., Gutiérrez, C., Gutiérrez, J. M., Güttler, I., Haensler, A., Halenka, T., Jerez, S., Jiménez-Guerrero, P., Jones, R. G., Keuler, K., Kjellström, E., Knist, S., Kotlarski, S., Maraun, D., van Meijgaard, E., Mercogliano, P., Montávez, J. P., Navarra, A., Nikulin, G., de Noblet-Ducoudré, N., Panitz, H-J., Pfeifer, S., Piazza, M., Pichelli, E., Pietikäinen, J-P., Prein, A. F., Preuschmann, S., Rechid, D., Rockel, B., Romera, R., Sánchez, E., Sieck, K., Soares, P. M. M., Somot, S., Srnec, L., Lund, Sørland, S. L., Termonia, P., Truhetz, H., Vautard, R., Warrach-Sagi K., and Wulfmeyer, V.: Regional climate downscaling over Europe: perspectives from the EURO-CORDEX community, Regional environmental change, 20, 1-20, doi:10.1007/s10113-020-01606-9, 2020.

Jain, S. K., Keshri, R., Goswami, A., and Sarkar, A.: Application of meteorological and vegetation indices for evaluation of drought impact: a case study for Rajasthan, India. Natural hazards, 54, 643-656. doi:10.1007/s11069-009-9493-x, 2010.

Jain, V. K., Pandey, R. P., Jain, M. K., and Byun, H. R.: Comparison of drought indices for appraisal of drought characteristics in the Ken River Basin, Weather and Climate Extremes, 8, 1-11, doi:10.1016/j.wace.2015.05.002, 2015.

Jia, Y., Zhang, B., and Ma, B.: Daily SPEI reveals long-term change in drought characteristics in Southwest China, Chinese Geographical Science, 28, 680-693, doi:10.1007/s11769-018-0973-3, 2018.

Katragkou, E., García-Díez, M., Vautard, R., Sobolowski, S., Zanis, P., Alexandri, G., Cardoso, R.M., Colette, A., Fernandez, J., Gobiet, A., and Goergen, K.: Regional climate hindcast simulations within EURO-CORDEX: evaluation of a WRF multi-physics ensemble, Geoscientific model development 8 603-618, doi:10.5194/gmd-8-603-2015, 2015.

Klein-Tank, A.M., Wijngaard, J.B., Können, G.P., Böhm, R., Demarée, G., Gocheva, A., Mileta, M., Pashiardis, S., Hejkrlik, L., Kern-Hansen, C. and Heino, R.: Daily dataset of 20th-century surface air temperature and precipitation series for the European Climate Assessment. International Journal of Climatology: A Journal of the Royal Meteorological Society, 22, 1441-1453, doi: 10.1002/joc.773, 2002.

Kobayashi, S., Ota, Y., Harada, Y., Ebita, A., Moriya, M., Onoda, H., Onogi, K., Kamahori, H., Kobayashi, C., Endo, H. and Miyaoka, K.: The JRA-55 reanalysis: General specifications and basic characteristics. Journal of the Meteorological Society of Japan. Ser. II, 93, 5-48, doi: 10.2151/jmsj.2015-001, 2015Kotlarski, S., Keuler, K., Christensen, O. B., Colette, A., Déqué, M., Gobiet, A., Goergen, K., Jacob, D., Lüthi, D., van Meijgaard, E., Nikulin, G., Schär, C., Teichmann, C., Vautard, R., Warrach-Sagi, K and Wulfmeyer, V.: Regional climate modeling on European scales: a joint standard evaluation of the EURO-CORDEX RCM ensemble, Geoscientific Model Development, 7(4), 1297-1333, doi:10.5194/gmd-7-1297-2014, 2014.

Lai, C., Zhong, R., Wang, Z., Wu, X., Chen, X., Wang, P., and Lian, Y,: Monitoring hydrological drought using long-term satellite-based precipitation data, Science of the total environment, 649, 1198-1208, doi:10.1016/j.scitotenv.2018.08.245, 2019

Li, J., Wang, Z., Wu, X., Xu, C. Y., Guo, S., and Chen, X.: Toward monitoring short-term droughts using a novel daily scale, Standardised antecedent precipitation evapotranspiration index, Journal of Hydrometeorology, 21(5), 891-908, doi:10.1175/JHM-D-19-0298.1, 2020.

Lima, D. C., Lemos, G., Bento, V. A., Nogueira, M., and Soares, P. M.: A multi-variable constrained ensemble of regional climate projections under multi-scenarios for Portugal–Part I: An overview of impacts on means and extremes, Climate Services, 30, 100351, doi:10.1016/j.cliser.2023.100351, 2023a.

Lima, D.C., Bento, V.A., Lemos, G., Nogueira, M. and Soares, P.M.: A multi-variable constrained ensemble of regional climate projections under multi-scenarios for Portugal–Part II: Sectoral climate indices. Climate Services, 30, 100377, https://doi.org/10.1016/j.cliser.2023.100377, 2023b.

Ma, B., Zhang, B., Jia, L., and Huang, H.: Conditional distribution selection for SPEI-daily and its revealed meteorological drought characteristics in China from 1961 to 2017, Atmospheric Research, 246, 105108, doi:10.1016/j.atmosres.2020.105108, 2020.

McKee, T. B., Doesken, N. J., and Kleist, J.: The relationship of drought frequency and duration to timescales, In Proceedings of the 8th Conference on Applied Climatology (Vol. 17, No. 22, pp. 179-183), 1993. https://climate.colostate.edu/pdfs/relationshipofdroughtfrequency.pdf (Last accessed on 30th July 2023)

Meyer, S. J., Hubbard, K. G., and Wilhite, D. A.: A crop-specific drought index for corn: I. Model development and validation, Agronomy Journal, 85(2), 388-395, doi:10.2134/agronj1993.00021962008500020040x, 1993.

Mishra, A. K., and Singh, V. P.: A review of drought concepts, Journal of hydrology, 391(1-2), 202-216, doi:10.1016/j.jhydrol.2010.07.012, 2010.

Moemken, J., Koerner, B., Ehmele, F., Feldmann, H. and Pinto, J.G.: Recurrence of drought events over Iberia. Part II: Future changes using regional climate projections. Tellus, 74, 262. doi:10.16993/tellusa.52, 2022.

Molina, M. O., Careto, J. A. M., Gutiérrez, C., Sánchez, E., and Soares, P. M. M.: The added value of high-resolution EURO-CORDEX simulations to describe daily wind speed over Europe, International Journal of Climatology, 43(2), 1062-1078, doi:10.1002/joc.7877, 2023.

Monish, N. T., and Rehana, S.: Suitability of distributions for standard precipitation and evapotranspiration index over meteorologically homogeneous zones of India, Journal of Earth System Science, 129, 1-19, doi:10.1007/s12040-019-1271-x, 2020.

Onuşluel Gül, G., Gül, A., and Najar, M.: Historical evidence of climate change impact on drought outlook in river basins: analysis of annual maximum drought severities through daily SPI definitions. Natural Hazards, 1-16, doi:10.1007/s11069-021-04995-0, 2021.

Palmer, W. C.: Meteorological drought (Vol. 30), US Department of Commerce, Weather Bureau, 1965. https://books.google.pt/books?hl=en&lr=&id=kyYZgnEk-L8C&oi=fnd&pg=PA6&dq=Palmer,+W.+C.,+(1965)+Meteorological+drought&ots=U4hAdh1Fom&sig=b_uhe6PC7FvMeofO1D9S59q7l64&redir_esc=y#v=onepage&q=Palmer%2C%20W.%20C.%2C%20(1965)%20Meteorological%20drought&f=false (Last accessed on 16th October 2023)

Pascoa, P., Russo, A., Gouveia, C. M., Soares, P. M., Cardoso, R. M., Careto, J. A., and Ribeiro, A. F.: A high-resolution view of the recent drought trends over the Iberian Peninsula, Weather and Climate Extremes, 32, 100320, https://doi.org/10.1016/j.wace.2021.100320, 2021.

Patel, N. R., Chopra, P., and Dadhwal, V. K.: Analyzing spatial patterns of meteorological drought using Standardised precipitation index, Meteorological Applications: A journal of forecasting, practical applications, training techniques and modelling, 14(4), 329-336, doi:10.1002/met.33, 2007.

Peel, M. C., Finlayson, B. L., and McMahon, T. A.: Updated world map of the Köppen-Geiger climate classification, Hydrology and earth system sciences, 11(5), 1633-1644, doi:10.5194/hess-11-1633-2007, 2007.

Pichelli, E., Coppola, E., Sobolowski, S., Ban, N., Giorgi, F., Stocchi, P., Alias, A., Belušić, D., Berthou, S., Caillaud, C. Cardoso, R.M. Chan, S., Christensen, O. B., Dobler, A., de Vries, H., Goergen, K., Kendon, E. J.,

Keuler, K., Lenderink, G., Lorenz, T., Mishra, A. N., Panitz, H-J., Schär, C., Soares, P. M. M., Truhetz, H. and Vergara-Temprado, J. The first multi-model ensemble of regional climate simulations at kilometer-scale resolution part 2: historical and future simulations of precipitation. Climate Dynamics, 56, 3581-3602, doi: 10.1007/s00382-021-05657-4, 2021.

Pohl, F., Rakovec, O., Rebmann, C., Hildebrandt, A., Boeing, F., Hermanns, F., Attinger, S., Samaniego, L., and Kumar, R.: Long-term daily hydrometeorological drought indices, soil moisture, and evapotranspiration for ICOS sites, Scientific Data, 10(1), 281, doi:10.1038/s41597-023-02192-1, 2023.

Prein, A. F., Gobiet, A., Truhetz, H., Keuler, K., Goergen, K., Teichmann, C., Maule, C. F., van Meijgaard, E., Déqué, M., Nikulin, G., Vautard, R., Coletter, A., Kjellström, E., and Jacob, D.: Precipitation in the EURO-CORDEX 0.11o and 0.44o simulations: high resolution, high benefits?, Climate dynamics, 46, 383-412, doi:10.1007/s00382-015-2589-y, 2016.

Rhee, J., Im, J., and Carbone, G. J.: Monitoring agricultural drought for arid and humid regions using multi-sensor remote sensing data, Remote Sensing of environment, 114(12), 2875-2887, doi: https://doi.org/10.1016/j.rse.2010.07.005, 2010.

Rios-Entenza, A., Soares, P. M., Trigo, R. M., Cardoso, R. M., and Miguez-Macho, G.:. Moisture recycling in the Iberian Peninsula from a regional climate simulation: Spatiotemporal analysis and impact on the precipitation regime, Journal of Geophysical Research: Atmospheres, 119(10), 5895-5912, doi:10.1002/2013JD021274, 2014.

Sánchez, E., Domínguez, M., Romera, R., López de la Franca, N., Gaertner, M.A., Gallardo, C. and Castro, M.: Regional modeling of dry spells over the Iberian Peninsula for present climate and climate change conditions: A letter. Climatic change, 107, 625-634, doi:10.1007/s10584-011-0114-9, 2011

Santos, J., Corte-Real, J., and Leite, S.: Atmospheric large-scale dynamics during the 2004/2005 winter drought in portugal, International Journal of Climatology: A Journal of the Royal Meteorological Society, 27(5), 571-586, doi:10.1002/joc.1425, 2007.

Seguí, P.Q., Martin, E., Sánchez, E., Zribi, M., Vennetier, M., Vicente-Serrano, S.M. and Vidal, J.P.: Drought: observed trends, future projections. The Mediterranean under climate change.123-131, doi: hal-01401386, 2016.

Shan, B., Verhoest, N.E. and De Baets, B. Identification of compound drought and heatwave events on a daily scale and across four seasons. Hydrology and Earth System Sciences, 28, 2065-2080, doi: 10.5194/hess-28-2065-2024, 2024.

Soares, P. M., and Cardoso, R. M.: A simple method to assess the added value using high-resolution climate distributions: application to the EURO-CORDEX daily precipitation, International Journal of Climatology, 38(3), 1484-1498, doi:10.1002/joc.5261, 2018.

Soares, P.M. and Lima, D.C.: Water scarcity down to earth surface in a Mediterranean climate: The extreme future of soil moisture in Portugal. Journal of Hydrology, 615, 128731, https://doi.org/10.1016/j.jhydrol.2022.128731, 2022.

Soares, P. M., Cardoso, R. M., Lima, D. C., and Miranda, P. M.: Future precipitation in Portugal: high-resolution projections using WRF model and EURO-CORDEX multi-model ensembles, Climate Dynamics, 49, 2503-2530, doi:10.1007/s00382-016-3455-2, 2017.

Soares, P.M., Lemos, G. and Lima, D.C.: Critical analysis of CMIPs past climate model projections in a regional context: The Iberian climate. International Journal of Climatology, 43(5), 2250-2270, https://doi.org/10.1002/joc.7973, 2023a.

Soares, P. M., Careto, J. A., Russo, A., and Lima, D. C.: The future of Iberian droughts: a deeper analysis based on multi-scenario and a multi-model ensemble approach, Natural Hazards, 1-28, doi:10.1007/s11069-023-05938-7, 2023b.

Singh, V. P., Guo, H., and Yu, F. X.: Parameter estimation for 3-parameter log-logistic distribution (LLD3) by Pome, Stochastic Hydrology and Hydraulics, 7, 163-177, doi:10.1007/BF01585596, 1993.

Spinoni, J., Vogt, J. V., Naumann, G., Barbosa, P., and Dosio, A.: Will drought events become more frequent and severe in Europe?, International Journal of Climatology, 38(4), 1718-1736, doi:10.1002/joc.5291, 2018.

Stagge, J. H., Tallaksen, L. M., Gudmundsson, L., Van Loon, A. F., and Stahl, K.: Candidate distributions for climatological drought indices (SPI and SPEI), International Journal of Climatology, 35(13), 4027-4040, doi:10.1002/joc.4267, 2015.

Svoboda, M. D., and Fuchs, B. A, () Handbook of drought indicators and indices (Vol. 2), Geneva, Switzerland: World Meteorological Organisation, 2016. https://www.droughtmanagement.info/literature/GWP_Handbook_of_Drought_Indicators_and_Indices_2016.pdf (Last accessed on 16th October 2023).

Thiemig, V., Gomes, G.N., Skøien, J.O., Ziese, M., Rauthe-Schöch, A., Rustemeier, E., Rehfeldt, K., Walawender, J.P., Kolbe, C., Pichon, D. and Schweim, C.: EMO-5: a high-resolution multi-variable gridded meteorological dataset for Europe. Earth System Science Data, 14, 3249-3272, doi:10.5194/essd-14-3249-2022, 2022.

Thornthwaite, C. W.: An approach toward a rational classification of climate. Geographical review 38:55–94, https://doi.org/10.2307/210739, 1948.

Tsakiris, G., and Vangelis, H. J. E. W.: Establishing a drought index incorporating evapotranspiration. European water, 9(10), 3-11, 2005. http://danida.vnu.edu.vn/cpis/files/Refs/Drought/Establishing%20a%20Drought%20Index%20Incorporating%20Evapotranspiration.pdf (Last accessed on 30th July 2023)

Umran Komuscu, A.: Using the SPI to analyze spatial and temporal patterns of drought in Turkey, Drought Network News (1994-2001), 49, 1999. https://digitalcommons.unl.edu/cgi/viewcontent.cgi?article=1048&context=droughtnetnews (Las accessed on 30th July 2023)

Van der Schrier, G., Jones, P. D., and Briffa, K. R.: The sensitivity of the PDSI to the Thornthwaite and Penman-Monteith parameterisations for potential evapotranspiration, Journal of Geophysical Research: Atmospheres, 116(D3), doi:10.1029/2010JD015001, 2011.

Vautard, R., Gobiet, A., Jacob, D., Belda, M., Colette, A., Déqué, M., Fernández, J., García-Díez, M., Goergen, K., Güttler, I., Halenka, T., Karacostas, T., Katragkou, E., Keuler, K., Kotlarski, S., Mayer, S., van Meijgaard, E., Nikulin, G., Patarčić, M., Scinocca, J., Sobolowski, S., Suklitsch, M., Teichmann, C., Warrach-Sagi, K., Wulfmeyer, V., and Yiou, P.: The simulation of European heat waves from an ensemble of regional climate models within the EURO-CORDEX project, Climate Dynamics, 41, 2555-2575, doi:10.1007/s00382-013-1714-z, 2013.

Vicente-Serrano, S. M.: Differences in spatial patterns of drought on different timescales: an analysis of the Iberian Peninsula, Water resources management, 20, 37-60, doi:10.1007/s11269-006-2974-8, 2006.

Vicente-Serrano, S. M., Beguería, S., and López-Moreno, J. I.: A multiscalar drought index sensitive to global warming: the Standardised precipitation evapotranspiration index, Journal of climate, 23(7), 1696-1718, doi:10.1175/2009JCLI2909.1, 2010.

Vicente-Serrano, S. M., Gouveia, C., Camarero, J. J., Beguería, S., Trigo, R., López-Moreno, J. I., Azorín-Molna, C., POasho, E., Lorenzo-Lacruz, J., Revuelto, J., Morán-Tejeda, E., and Sanchez-Lorenzo, A.: Response of vegetation to drought time-scales across global land biomes, Proceedings of the National Academy of Sciences, 110(1), 52-57, doi:10.1073/pnas.1207068110, 2013.

Wan, L., Bento, V.A., Qu, Y., Qiu, J., Song, H., Zhang, R., Wu, X., Xu, F., Lu, J. and Wang, Q.: Drought characteristics and dominant factors across China: Insights from high-resolution daily SPEI dataset between 1979 and 2018. Science of The Total Environment, 901, 166362, https://doi.org/10.1016/j.scitotenv.2023.166362, 2023.

Wang, Q., Wu, J., Lei, T., He, B., Wu, Z., Liu, M., MO, X., Geng, G., Li, X., Zhou, H., and Liu, D.: Temporal-spatial characteristics of severe drought events and their impact on agriculture on a global scale, Quaternary International, 349, 10-21, https://doi.org/10.1016/j.quaint.2014.06.021, 2014.

Wang, Q., Shi, P., Lei, T., Geng, G., Liu, J., Mo, X., Li X, Zhou, H., and Wu, J.: The alleviating trend of drought in the Huang-Huai-Hai Plain of China based on the daily SPEI, International Journal of Climatology, 35(13), 3760-3769, doi:10.1002/joc.4244, 2015.

Wang, Q., Wu, J., Li, X., Zhou, H., Yang, J., Geng, G., An, X., Liu, L., and Tang, Z.: A comprehensively quantitative method of evaluating the impact of drought on crop yield using daily multi-scale SPEI and crop growth process model, International journal of biometeorology, 61, 685-699, doi:10.1007/s00484-016-1246-4, 2017.

Wang, Q., Zeng, J., Qi, J., Zhang, X., Zeng, Y., Shui, W., Xu, Z., Zhang, R., Wu, X., and Cong, J.: A multi-scale daily SPEI dataset for drought characterisation at observation stations over mainland China from 1961 to 2018, Earth System Science Data, 13(2), 331-341, doi:10.5194/essd-13-331-2021, 2021.

Wang, Q., Zhang, R., Qi, J., Zeng, J., Wu, J., Shui, W., Wu, X., and Li, J.: An improved daily Standardised precipitation index dataset for mainland China from 1961 to 2018, Scientific Data, 9(1), 124, doi:s41597-022-01201-z, 2022.

Wells, N., Goddard, S., and Hayes, M. J.: A self-calibrating Palmer drought severity index. Journal of climate, 17(12), 2335-2351, doi:10.1175/1520-0442(2004)017<2335:ASPDSI>2.0.CO;2, 2004.

Wilhite, D. A.: Drought as a natural hazard: concepts and definitions, Drought Mitigation Center Faculty Publications, University of Nebraska, Lincoln, 2000. https://digitalcommons.unl.edu/cgi/viewcontent.cgi?article=1068&context=droughtfacpub (Last accessed on 30th July 2023)

Wilhite, D. A.: Drought and water crises: science, technology, and management issues, Crc Press, 2005. https://books.google.pt/books?hl=en&lr=&id=D0puBwAAQBAJ&oi=fnd&pg=PP1&dq=Wilhite,+D.+A.,+(2005)+Drought+and+water+crises:+science,+technology,+and+management+issues,+Crc+Press.&ots=hxDQOUtG0h&sig=VbEqYSzPs42cxdIXIYu0RX-IZaE&redir_esc=y#v=onepage&q=Wilhite%2C%20D.%20A.%2C%20(2005).%3A%20Drought%20and%20water%20crises%3A%20science%2C%20technology%2C%20and%20management%20issues%2C%20Crc%20Press.&f=false (Last accessed on 16th October 2023).

Wilhite, D. A., and Glantz, M. H.: Understanding: the drought phenomenon: the role of definitions, Water international, 10(3), 111-120, doi:10.1080/02508068508686328, 1985.

Wu, H., Hayes, M. J., Weiss, A., and Hu, Q. I.: An evaluation of the Standardised Precipitation Index, the China-Z Index and the statistical Z-Score, International Journal of Climatology: A Journal of the Royal Meteorological Society, 21(6), 745-758, doi:10.1002/joc.658, 2001.

Xie, P., Chen, M., Yang, S., Yatagai, A., Hayasaka, T., Fukushima, Y. and Liu, C.: A gauge-based analysis of daily precipitation over East Asia. Journal of Hydrometeorology, 8(3), pp.607-626, doi:10.1175/JHM583.1, 2007.Zhang, Y., and Li, Z.: Uncertainty analysis of Standardised precipitation index due to the effects of probability distributions and parameter errors, Frontiers in Earth Science, 8, 76, doi:10.3389/feart.2020.00076, 2020.

Zhang, R., Bento, V. A., Qi, J., Xu, F., Wu, J., Qiu, J., Li, J., Shui, W., and Wang, Q.: The first high spatial resolution multi-scale daily SPI and SPEI raster dataset for drought monitoring and evaluating over China from 1979 to 2018., Big Earth Data, 1-26, doi:10.1080/20964471.2022.2148331, 2023.

Zhang, X., Duan, Y., Duan, J., Jian, D., and Ma, Z.: A daily drought index based on evapotranspiration and its application in regional drought analyses, Science China Earth Sciences, 1-20, doi:10.1007/s11430-021-9822-y, 2022a.

Zhang, X., Duan, Y., Duan, J., Chen, L., Jian, D., Lv, M., Yang, Q., and Ma, Z.: A daily drought index-based regional drought forecasting using the Global Forecast System model outputs over China, Atmospheric Research, 273, 106166, https://doi.org/10.1016/j.atmosres.2022.106166, 2022b.

Zscheischler, J., Martius, O., Westra, S., Bevacqua, E., Raymond, C., Horton, R.M., van den Hurk, B., AghaKouchak, A., Jézéquel, A., Mahecha, M.D., Maraun, D., Ramos, A., Ridder, N. N., Thiery, W. and Vignotto, E. A typology of compound weather and climate events. Nature reviews earth & environment, 1, 333-347, doi: s43017-020-0060-z, 2020.